Identification of MH370 Route into the Southern Indian Ocean

Bobby Ulich, Ph.D., M.S., B.S.

7 March 2018

1. Summary

Four years ago today, at a time between 18:29 and 19:41 UTC on 7 March 2014, Malaysia Airlines Flight MH370 made a turn to the south and flew into the Southern Indian Ocean (SIO) until it ran out of fuel and fell into the sea. In this paper I present a new analysis of the Inmarsat satellite data [1] that identifies a unique flight path curving eastward during the period from 19:41 UTC on 7 March 2014 until 00:19 UTC on 8 March 2014, when the last satellite data were recorded shortly before the impact occurred near the "7th Arc".

I have analyzed all five possible autopiloted methods available for lateral navigation [2] [3] by applying matched-filter detection methods. My analysis provides positive indication that no fully acceptable solutions exist for four of the five autopiloted lateral navigation methods. Furthermore, my analysis demonstrates there is only one solution for the fifth method – a Constant Magnetic Track at 181.2 degrees, most likely produced by a TRACK HOLD command when on a 180.0° true track between waypoints AGEGA and BULVA with a 15 NM right lateral offset.

The predicted location of the aircraft debris field is 31.57°S, 96.77°E. This location is outside and north of the 25,000 km^2 Site 1 search zone proposed by the ATSB [4]. It lies well north of the Diamantina Escarpment, in the Site 2 Extension Area 3, as shown in the Government of Malaysia map in Figure 1 [5].

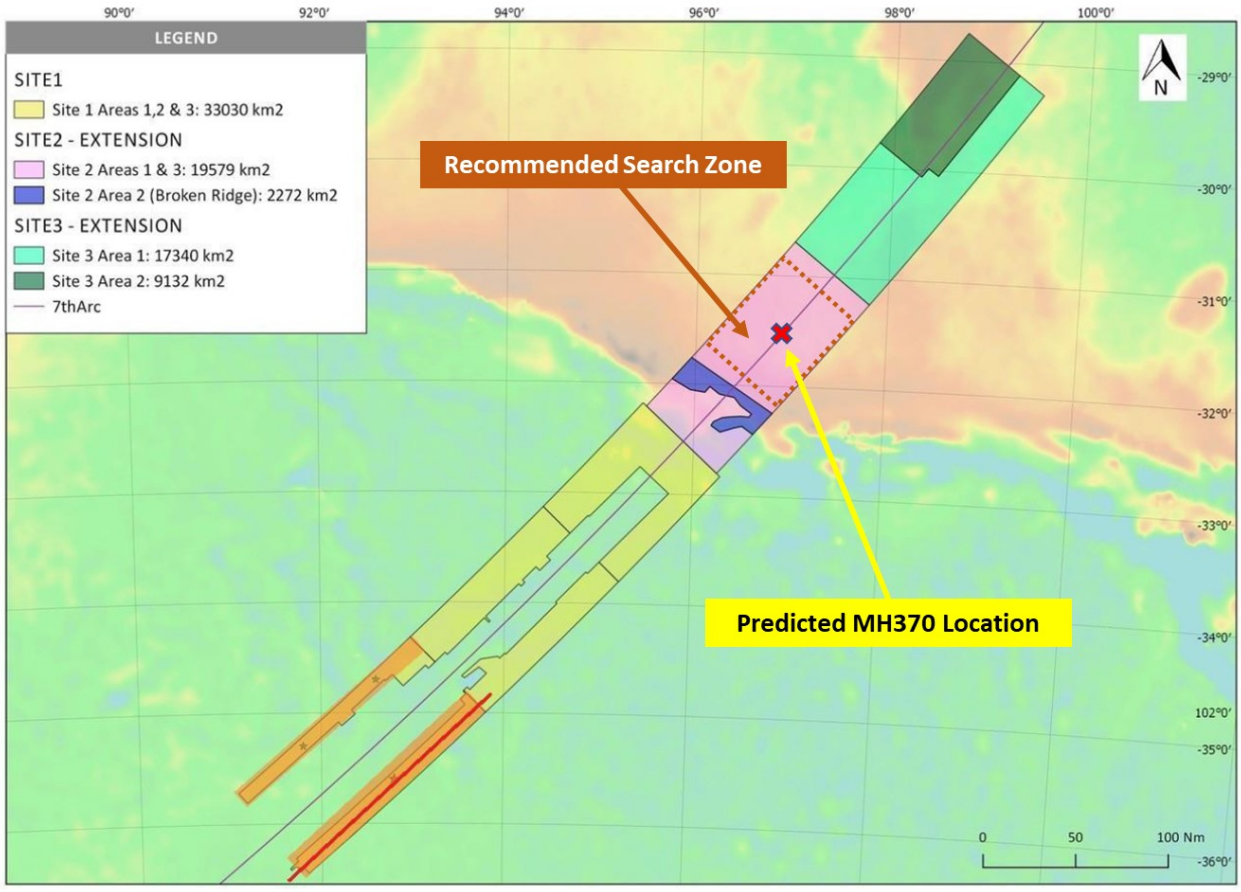

Figure 1. Map of Search Sites and Predicted MH370 Location

In summary:

(1) The very high, and accelerating, rates of descent required to match the 00:19:29 and 00:19:37 Burst Frequency Offsets (BFOs) indicate the aircraft crashed very near the 7th Arc (quite possibly within 10 NM, and almost certainly within 25 NM).
(2) The previous searches were unsuccessful near the 7th Arc south of 32.85°S latitude [4].
(3) The aircraft must, therefore, be very near the 7th Arc but north of 32.85°S latitude.
(4) This conclusion, based partly on previous unsuccessful search results, is confirmed by my new analysis, which is independent of previous search results.
(5) Only one lateral navigation method (181.2° Constant Magnetic Track, or CMT) is fully consistent with the Inmarsat satellite data from 19:41-00:11, the NOAA GDAS weather data [6] [7] [8], and the B777-200ER autopilot capabilities.
(6) This best-fit SIO route is flown at FL335 using Maximum Range Cruise air speed.
(7) The 181.2° CMT can be produced by the flight crew entering TRACK HOLD using the Mode Control Panel when 9M-MRO was on a 180.0° true track.
(8) This 181.2° CMT route originates within 1 NM of the north-south line 15 NM west of waypoints AGEGA to BULVA.
(9) Initiating a TRACK HOLD on the offset AGEGA-to-BULVA line results in a magnetic track that is within 0.05° of that of the post-19:41 best-fit CMT route.
(10) The right lateral offset path from AGEGA to BULVA is consistent with a continuation of the 15 NM right lateral offset Contingency Procedure previously performed by 9M-MRO at 18:25 [9] parallel to Airway N571 between MEKAR and IGOGU.
(11) The identified MH370 SIO Route has a predicted terminus well north of the previously searched area, at latitude 31.57°S on the 7th Arc.

The matched-filter method I used for route searches, and the derived MH370 SIO Route parameters, are discussed in detail in this paper. Recommendations for a new priority search zone (± 25 NM wide and ± 30 NM long) are presented (see Figure 1). I hope this new ≈ 10,000 km^2 area will be searched by Ocean Infinity, and that the 9M-MRO debris field will be successfully located.

TABLE OF CONTENTS

2. Autopiloted Flight after the Final Major Turn (FMT)

2.1 Satellite Data

The relevant Inmarsat satellite data for MH370 [1] that may be used to determine the MH370 SIO Route are shown in Table 1 in the yellow cells. There are five pairs of Burst Timing Offsets (BTOs) and Burst Frequency Offsets (BFOs) between 19:41–00:11 that may be used for this purpose, for a total of ten data points at five specific times. Therefore, there are only 15 numbers from the satellite data from which to determine the SIO route. I chose to use the 00:19:37 data as the 7th Arc, rather than the 00:19:29 data, because the uncertainty in the BTO at 00:19:37 is much smaller. The choice of using one or the other, or both, of those last two data points is immaterial to the route fitting process and to the predicted aircraft location, when considering other uncertainties. The aircraft speed and track from 00:11–00:19 are sufficiently uncertain due to fuel exhaustion occurring in that period of time that only the data up to 00:11 (the 6th Arc) are used for the MH370 SIO Route determination, although the 00:19 data are subsequently used in predicting the 7th Arc location by continuing that route.

Table 1 shows how the "raw" BTOs and BFOs measured by Inmarsat are corrected (i.e., "calibrated") for two minor effects. The corrections are (1) channel-to-channel bias frequency differences and (2) a small frequency correction at 00:19 for thermal warm-up of the reference frequency oscillator in the Satellite Data Unit (SDU) [9]. This process produces the "Calibrated" BTO and BFO (i.e., CBTO and CBFO) values I use for route fitting.

The yellow cells in Table 1 include the 5 pairs of CBTOs/CBFOs that I used to determine the SIO route. Along with the 5 handshake times, these 10 numbers are the primary inputs to the route fitting program, which generally produces 12 outputs – 5 pairs of latitude/longitude positions plus an air speed and a route bearing. Although the number of fitted parameters (12) exceeds the number of data points (10) being fitted, the bearing and air speed are dependent on the best-fit positions, so the effective number of independent fitted parameters is actually just 10.

The blue cells in Table 1 are the 7th Arc CBTO and CBFO. These are used by the Route Fitter, after the SIO Route is determined based on the 19:41-00:11 data, to predict the 00:19:37 latitude and longitude and Rate of Descent (ROD). This 7th Arc position is taken as the predicted location of the aircraft debris field.

2.2 No Maneuvers After 19:41

Figure 2 and Figure 3 show the relevant "calibrated" BTO and BFO data, respectively, from Table 1.

Based on the satellite data in Figure 2 and Figure 3, it appears highly likely that the aircraft made no maneuvers, after the Final Major Turn (FMT), from 19:41–00:11. A maneuver is a change in:

(1) lateral navigation method (or a change in the commanded bearing or waypoint using the same lateral navigation method),
(2) air speed, or
(3) altitude.

Maneuvers must be instigated by a pilot entering commands into the Flight Management Computer (FMC) or the Mode Control Panel (MCP), which are components of the Autopilot Flight Director System (AFDS).

The CBTOs (shown in Figure 2) depend on the line-of-sight distance of the aircraft from the geostationary satellite (Inmarsat-3F1). This plot displays a high degree of smoothness. The dashed line is a cubic polynomial fitted to the CBTO values. If there were major turns or speed changes made after 19:41, the slope of the BTO plot would be discontinuous. Based on Figure 2, there were no abrupt turns or major speed changes at any point from 19:41-00:11. However, very slow turns due to a curving route over a period of hours are allowed by Figure 2, as are minor speed or altitude changes occurring slowly over time.

Table 1. Inmarsat Satellite Data Used in This Analysis

			UTC	**19:41:02.9**	**20:41:04.9**	**21:41:26.9**	**22:41:21.9**	**0:10:59.9**	**0:19:37.4**
			Date	**7 March 2014**				**8 March 2014**	
Calibrated Burst Frequency Offset (CBFO) (Calibrated for channel Fixed Frequency Bias and OCXO transient)	**"Raw" BFO from Inmarsat Log**		**Hz**	**111**	**141**	**168**	**204**	**252**	**-2**
	Transmit Channel Type and Number			**R4**	**R4**	**R4**	**R4**	**R4**	**R10**
	$\Delta_{channel}$ (difference in Fixed Frequency Bias w.r.t. 150.27 Hz)		**Hz**	**0.4**	**0.4**	**0.4**	**0.4**	**0.4**	**-0.2**
	Δ_{OCXO} (SDU warmup transient correction)		**Hz**	**---**	**---**	**---**	**---**	**---**	**-3**
	"Calibrated" BFO (all with FFB = 150.27 Hz)		**Hz**	**111.4**	**141.4**	**168.4**	**204.4**	**252.4**	**-5.2**
	Estimated 2-σ Error in CBFO	**Noise and Drift**	**Hz**	**6.0**	**6.0**	**6.0**	**6.0**	**6.0**	**6.0**
		Relative Channel Offset Calibration	**Hz**	**0.0**	**0.0**	**0.0**	**0.0**	**0.0**	**0.0**
		OCXO Warmup Transient Correction	**Hz**	**---**	**---**	**---**	**---**	**---**	**2**
		Total Error = Root Sum of Squares	**Hz**	**6.0**	**6.0**	**6.0**	**6.0**	**6.0**	**6.3**
Calibrated Burst Timing Offset (CBTO) (Corrected for timing offsets per Inmarsat & ATSB)	**"Raw" BTO from Inmarsat Log**		**μs**	**11,500**	**11,740**	**12,780**	**14,540**	**18,040**	**49,660**
	Receive Channel			**R1200**	**R1200**	**R1200**	**R1200**	**R1200**	**R1200**
	Δ_{BTO} (timing correction per Inmarsat & ATSB)		**μs**						**-31,250**
	"Calibrated" BTO		**μs**	**11,500**	**11,740**	**12,780**	**14,540**	**18,040**	**18,410**
	2-σ Error (from DSTG)		**μs**	**58**	**58**	**58**	**58**	**58**	**86**
Notes on Message Type and Corrections Applied				**Handshake # 2**	**Handshake # 3**	**Handshake # 4**	**Handshake # 5**	**Handshake # 6**	**Handshake #7B; BTO correction = -4/128 s**

The CBFOs in Figure 3 are smooth and surprisingly linear with time. They depend on the horizontal component of the velocity of the aircraft projected toward the satellite. This dependence is actually quite complex, because the Doppler shift is (mostly) compensated by the SDU, using an assumed nominal satellite location. Because the satellite is never actually at this nominal fixed location, the CBFOs are not completely compensated for the Doppler shift caused by the aircraft's horizontal speed. The CBFOs do contain limited information on the aircraft location, horizontal ground speed, and direction of travel (i.e., the true track).

The Doppler shift due to vertical speed of the aircraft is uncompensated by the SDU in the aircraft, and the component of vertical speed projected toward the actual satellite location directly affects the BFO. This vertical speed appears to dominate at 00:19 (see the last two CBFOs, colored red, on the right side of Figure 3). These are the last two BFOs after Main Engines Fuel Exhaustion (MEFE) occurred circa 00:17:30 [10]. The rapidly declining BFOs circa 00:19 indicate an increasingly rapid aircraft descent after fuel exhaustion occurred.

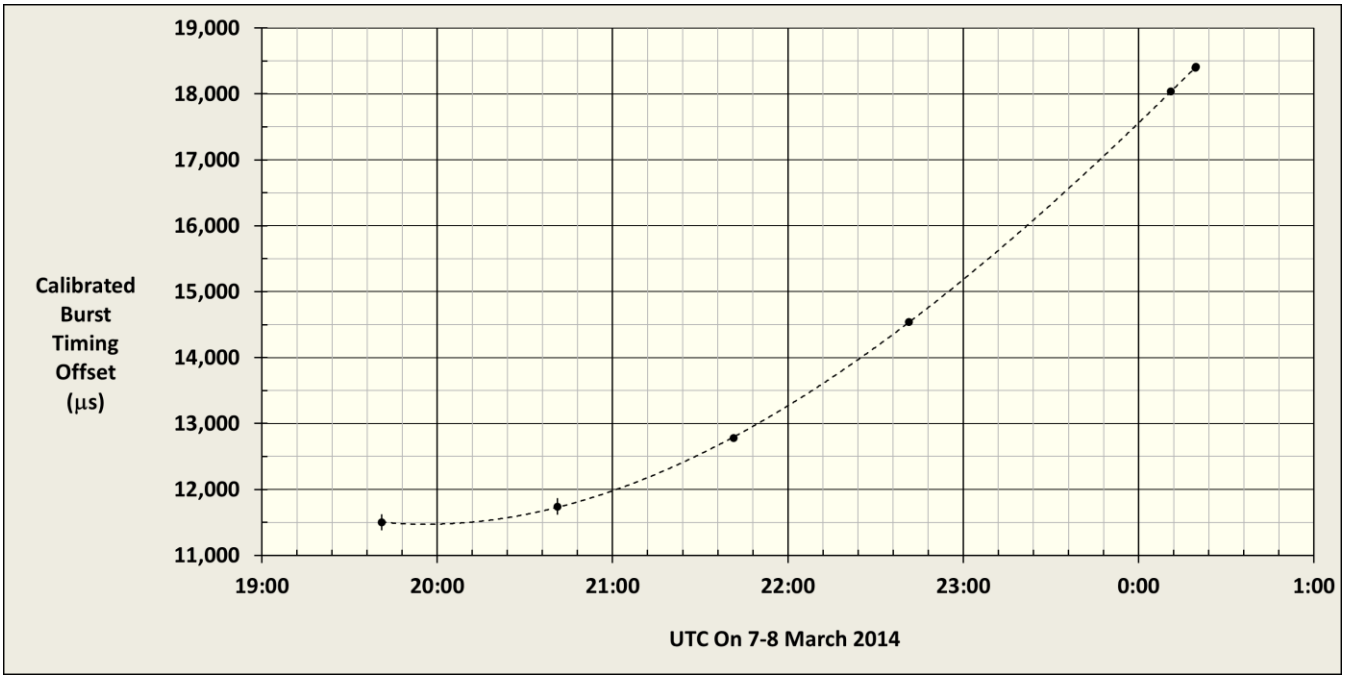

Figure 2. Calibrated Burst Timing Offset (CBTO) Data for the SIO Route

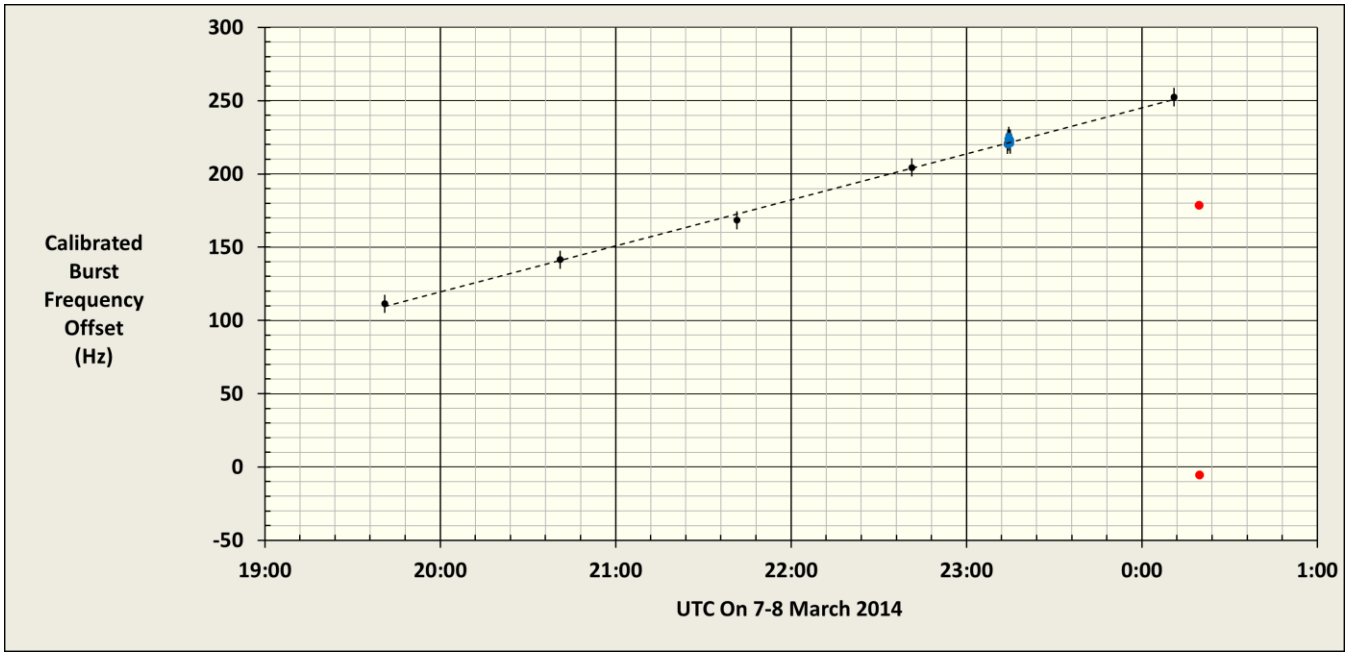

Figure 3. Calibrated Burst Frequency Offset (CBFO) Data for the SIO Route

2.3 SIO Route Fitting Assumptions Based on the Satellite Data

At the "handshake" times from 19:41 to 00:11, the SDU in the aircraft communicated with the Inmarsat ground station in Perth, Australia through the geostationary satellite link. Data were recorded during each network log-on process. The plot of these "handshake" CBFOs in Figure 3 is quite smooth and linear. It does not indicate that significant turns, or changes in altitude or speed, occurred during this time period, which would lead to steps, up or down, in the CBFOs. If there were a significant maneuver of any sort, the CBFO plot would show a step change in value, and it does not. The absence of such steps in BFO value supports three assumptions being made for the time period from 19:41-00:11:

(1) constant flight level,
(2) constant lateral navigation method and course setting, and
(3) slowly varying air speed.

In this context, a "constant lateral navigation method and course setting" means that neither the type of lateral navigation method nor the setting used (for example, 180.0 degrees True Track, or a waypoint for LNAV) were changed by a human from 19:41–00:11.

Based on the CBTO and CBFO plots in Figure 2 and Figure 3, there is no evidence of manual flying or maneuvers from 19:41-00:11. These observations leads to one additional assumption: the air speed control method was unchanged from 19:41 – 00:11.

In summary, based on the satellite data:

(1) MH370 was autopiloted from 19:41–00:11,
(2) at a constant flight level,
(3) using a single air speed control method and setting (Cost Index, or Mach, or KIAS), and
(4) using a single lateral navigation method and setting (bearing or waypoint).

Note that I have plotted the second phone call CBFOs at 23:14 in Figure 3 in blue. However, I have not included them in Table 1 or used them to fit the MH370 SIO Route. The reason for this is that they have an unknown frequency offset relative to the other transmitting channels used, so they should not be used for SIO route fitting, even though they appear fairly consistent with the other CBFOs in Figure 3 because the relevant channel bias frequency difference is apparently small.

3. All Assumptions Used in Fitting the SIO Route to the Inmarsat Data

I have analyzed the satellite data set in Table 1, assuming autopiloted flight at constant altitude/speed/lateral navigation from 19:41 to 00:11, to discern the values of altitude, speed, and course. Previously I developed generalized models that predict air speed, fuel flow, and endurance for a B777-200ER aircraft, like 9M-MRO, with Rolls Royce Trent 892B engines [11, 12, 13]. These three models are used in this analysis. I also used the NOAA Global Data Assimilation System (GDAS) weather data [6] [7] [8] as a function of latitude and longitude (every 1°), atmospheric pressure level (about every 4,000 feet of altitude), and time (every 3 hours). I interpolated the GDAS air temperature and wind data in these four dimensions at points along the route.

I also found the best air speed control modes and flight levels to match both the CBTO/CBFO data and the known endurance based on the estimated Main Engines Fuel Exhaustion (MEFE) time of 00:17:30 on 8 March 2014 [10].

In this MH370 SIO Route analysis I made the following assumptions:

(1) After the FMT, the aircraft flight path was automatically controlled by the AFDS (i.e., the autopilot was used) with no settings altered by a human after 19:41.
(2) The FMC/MCP navigated laterally in a standard control mode and setting without degradation or change.
(3) One air speed control mode (and setting, if needed) was used.
(4) The flight level was constant.
(5) The weather data (air temperature and wind at altitudes of interest) from NOAA GDAS are accurate within the normal uncertainties ($1\sigma \leq 1$ C for Static Air Temperature and ≤ 5.7 kts RMS for each of two orthogonal winds [14]).
(6) The engines performed normally with Air Packs On.
(7) The Performance Degradation Allowance (PDA) given in the MH370 Flight Plan [15] (average of both engines of 1.5%) is accurate.
(8) There was no "aerodynamic" damage to the aircraft prior to MEFE that would increase drag.

(9) The Auxiliary Power Unit (APU) was not started prior to MEFE.

4. Route Fitting Metrics

The route-fitting process seeks to optimize the differences between the measured and predicted CBTOs and CBFOs. Optimization is not the same as minimization. The differences between the measured and the predicted values are the "residual errors" of the route fit. An optimum fit has residual errors which have the same dispersion as the expected standard deviations. I use the root-mean-square (RMS) as the measure of dispersion because the standard deviation only indicates the dispersion about the mean value, which might not be zero, especially when there are systematic route errors. In this case, the mean CBTO and CBFO errors should be close to zero, and I also want the dispersion to match the expected values. The RMS function can be used to accomplish both, since it represents a combination of mean error and standard deviation.

My Objective Function, which is minimized by the Route Fitter, is a nonlinearly-weighted RMS of normalized residual errors. Each error statistic is "normalized" by dividing it by its corresponding expected value. The weighting functions are identical (except for a multiplicative scalar), being linear above 1.0 normalized error and highly nonlinear below 1.0. They have a very steep "cliff" at about 0.9 normalized error value, so that errors smaller than this are very lightly weighted. For simplicity, I take the RMS normalization value to be equal to the known standard deviation, which will be the case when the mean value is close to zero near convergence when fitting the correct route.

4.1 Normalized CBTO Residual Errors

The expected standard deviation of the CBTO errors is 29 μs [16]. I define the normalized CBTO RMS error as follows:

(1) $\Sigma_{CBTO} \equiv$ RMS(CBTO Residuals) / 29 μs ,

where the RMS function of parameter "X" is simply the square root of the mean of the squares of N residuals "X_i":

(2) $RMS(X) \equiv [\ SUM(\ X_i^2\ )/N\ ]^{1/2}$.

4.2 Normalized CBFO Residual Errors

The CBFOs have a standard deviation (1σ) of about 4.3 Hz when 20 flights are analyzed as one ensemble with outliers excluded [17]. I know that frequency drifts occur, since there is an automated calibration process built into the SDU to compensate that drift. The calibration process adjusts the frequency offset occasionally (> 1 day), and it made a correction of 16 Hz when MH370 was at the gate at KLIA. Therefore, it seems reasonable to expect small drifts of at least several Hz to occur between flights (and between corrections), and this effect broadens the dispersion of the BFOs when many flights are included in the BFO statistic. Taking this slow drift into account, I would expect the BFOs to vary less than 4.3 Hz 1σ over the approximately 5 hours from 19:41-00:11. In this analysis, I use a RMS value of 3.0 Hz for the expected dispersion of the CBFOs. This value closely matches that best-fit value for the correct MH370 SIO Route, as I shall demonstrate later in this paper.

The normalized CBFO residual error statistic is:

(3) $\Sigma_{CBFO} \equiv$ RMS(CBFO Residuals) / 3.0 Hz .

4.3 Goodness of Fit Metric

I use an overall figure of merit, which I call the Goodness of Fit (GOF), for evaluating candidate routes. GOF is the unweighted RMS of the normalized residual CBTO and CBFO RMS errors. The GOF is simply:

(4) Goodness of Fit = GOF $\equiv \{\ [\ (\Sigma_{CBTO})^2 + (\Sigma_{CBFO})^2\ ]\ /\ 2\ \}^{1/2}$.

When the "correct" route is fitted, its normalized CBTO and CBFO errors will each be very close to 1.0, so the GOF will also be 1.0. A route fit with GOF = 1.0 generally means excellent consistency with the expected noise statistics of the satellite data.

A GOF $\gg$ 1 indicates a poor fit because the route is not the correct one, and systematic errors exist.

A GOF $\ll$ 1 also indicates a poor fit, because the route parameters are being strongly affected (i.e., contaminated) by the noise in the satellite data, reducing the best-fit normalized BTO and BFO residuals below 1.0.

The task at hand, then, is to search for a route that has GOF = 1.0, when adjacent routes, both at nearby smaller and at nearby larger bearings, have a GOF < 1. Despite the presence of noise in the satellite data, I can search for, and identify, the "correct" route by testing the best-fit CBTO/CBFO residuals to see if they have noise statistics which match their known/expected values. Nearby bearings should have smaller residuals, particularly the CBTO residuals. Generally speaking, I do not expect to see a significant change in the RMS CBFO error with small changes in bearing, because the CBFOs are inherently insensitive to small course changes due to the pre-compensation in frequency applied by the SDU. The RMS CBTO residuals are the primary indicator of route "correctness" when considering small course changes. If the CBTO residuals are too high ($\Sigma_{CBTO} > \approx 1.2$), the route is incorrect. If they are too low ($\Sigma_{CBTO} < \approx 0.8$), the route could possibly be near the correct route, but it cannot be the correct route because the fitted route parameters are being contaminated by CBTO noise, leading to residuals that are too small.

4.4 Uncertainty in Estimated Statistical Properties

It should also be noted that the estimates of the statistical properties of the fitting residuals for a single route are noisy because most are based on only 10 data points. The relative error in the estimate of the statistical parameters (RMS) is approximately $10^{-1/2} = 32\%$ of the standard deviation. So, it is no surprise that there are some differences between best-fit residuals for a single route and the statistical properties (of BFO, BTO) based on many data points from many previous flights. On the other hand, the bias of the estimated statistical parameter is correlated for all route trials I have done because they all use the same data set for MH370. That correlation means that differences in estimated statistical properties are meaningful at a level where the differences are smaller than 32%. Very small differences in residual RMS values of only a few per cent are probably not meaningful in indicating a preference of one route over another. Since I have 2 statistical parameters contributing to the GOF, the noise level of the GOF with independent data sets (i.e., different data from different flights) will be $2^{-1/2}$ times the noise in a single parameter, or about ± 22% overall. Fitting different routes to a single data set is different because the same data are used. That biases the statistical estimates, but by nearly the same amount for each trial. Thus, I can actually do rather well in comparing different route trials operating on the same data set. The absolute statistics will be incorrect due to unknown bias (caused by the small-number statistics of the data set), but since the bias depends on the data set, and not on the trial parameters, I can extract useful information from GOF differences which may be smaller than the unknown bias.

5. Computer Models Used in Route Fitting

5.1 BTO and BFO Models

The BTO and BFO computer models I built [18] follow the form and parameters suggested by ATSB [19] and Inmarsat [20]. Comparisons with several independently-built models, including one used by the Defense Science and Technology Group, confirm precise agreement and validate their accuracy.

5.2 Magnetic Variation Model

For fitting routes with magnetic bearing references, I use the same 1 January 2005 epoch for the magnetic variation (also called magnetic declination) database as used in 9M-MRO [21]. I use the NOAA magnetic variation database and interpolate a table with values every 1° in latitude and longitude [22].

5.3 Air Speed and Fuel Flow Models

I have built a computer model of the air speed control modes used in B777 aircraft [11] [12] [13]. This model predicts the air speed (in Mach, TAS, and KIAS) and the fuel flow for each of the standard speed control modes, taking into account the flight level, air temperature, and aircraft weight. I assume the AFDS controls the air speed using auto-throttle. There are one or two "free" AFDS parameters that establish the nominal air speed profile, and non-standard air temperature will also affect the true air speed. The first parameter is the air speed control mode, which can be one of the following:

(1) ECON with a Cost Index,
(2) Long Range Cruise (LRC),
(3) Maximum Range Cruise (MRC),
(4) Holding,
(5) constant KIAS (in 1 knot steps), or
(6) constant Mach (in 0.01 steps).

For constant Mach/KIAS, a second parameter (the "setting") must also be specified (Mach or Knots Indicated Air Speed). For ECON mode, I used Cost Index = 52 for this analysis because that is the Flight Plan value [15], which was used in the early cruise stage of MH370 up to the Diversion circa 17:22.

5.4 Final Major Turns (FMT) Model

My FMT computer model begins at 18:20:00 when 9M-MRO was on the military radar track. It allows up to 10 maneuvers to be programmed. Each maneuver is specified in time and action (change in altitude, change in speed, or change in true track). The FMT Model computes position, altitude, speed, and course every 1 second from 18:20 – 19:00. Turn rates are limited by the maximum allowable bank angle, which is speed dependent. The FMT Model also compares predicted and observed CBTOs and CBFOs in this time period so that the maneuver parameters may be optimized. This includes the 15 NM right lateral offset Contingency Procedure performed circa 18:25 [9].

5.5 End-of-Flight Model

I have built a computer model for the end-of-flight aircraft parameters, beginning at the first (right) engine fuel exhaustion. Based on simulator results, the airspeed first declines until a point is reached where a descent begins that holds the indicated air speed constant. That descent continues until either (a) an altitude is reached where the remaining (left) engine can maintain Engine Inoperative air speed, or (b) the left engine also reaches fuel exhaustion. In the case of MH370, the left engine flamed out when the initial controlled descent was near the maximum altitude for level flight with an Engine Inoperative. When the second (left) engine stopped producing thrust due to fuel exhaustion, the descent steepened and the horizontal deceleration increased. My End-of-Flight Model utilizes two different slow-down rates, depending on the number of flamed-out engines.

Figure 4 shows the predicted primary aircraft parameters during the fuel exhaustion events.

Based on my analysis of fuel flow sensor readings during a prior flight (kindly provided by ATSB), the right engine in 9M-MRO had 2.1% higher fuel flow than the left engine when cruising. This caused the right engine to flame out circa 00:09:30, approximately 8 minutes before the left engine flame-out at 00:17:30 [10]. Thus, the right engine flamed out approximately 1.5 minutes before the 6th Arc handshake at 00:11:00, and 9M-MRO had already begun to slow down before reaching the 6th Arc.

I used my End-of-Flight Model to predict the average ground speed between 00:11 and 00:19 UTC for the purpose of fitting the last leg from the 6th Arc to the 7th Arc. The flight level at 00:19:37 predicted by my End-of-Flight Model (see Figure 4) is about FL230. However, after 00:17:30 (MEFE), my End-of-Flight Model does not accurately predict the aircraft behavior, including the time of impact.

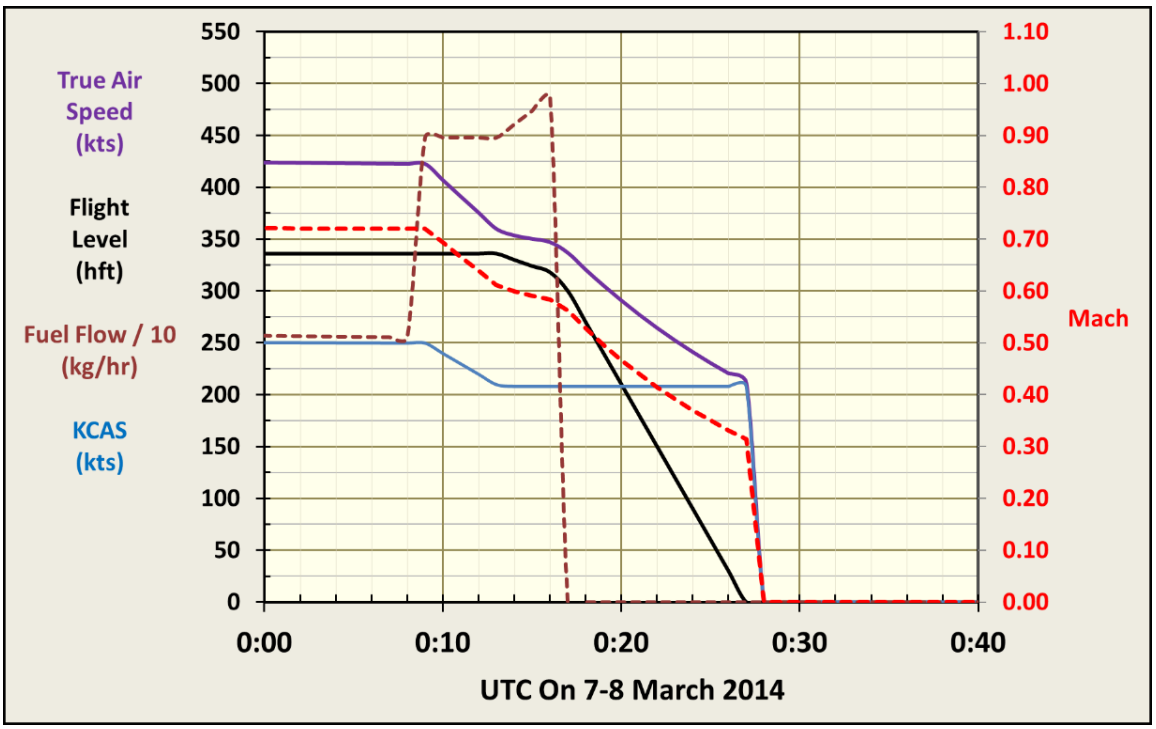

Figure 4. End-of-flight Model Parameters

When the Ram Air Turbine (RAT) deploys after MEFE, with little or no hydraulic power, the B777 tends to roll to the left [23]. This roll may have developed into a fairly steep descent, consistent with the ≈ 15,000 fpm indicated by the 00:19:37 BFO and with the lack of the expected next SDU transmission at 00:21.

6. Lateral Navigation

6.1 Direction Versus Destination

In the lateral navigation methods not using waypoints, the direction of the future path is specified, not the destination. Only the waypoint navigation mode using the FMC LNAV function is a "destination-driven" route with position feedback along the way [3]. One must specify an end point in order to compute the geodesic (great circle) path, which is the shortest distance to that waypoint. The LNAV function to a waypoint follows a specific ground track, and drifts off that track are sensed by the GPS/ADIRU and are corrected in real time. Cross-track navigation errors do not accumulate in LNAV when using waypoints. However, in the direction-driven lateral navigation modes, the deviations off a theoretical course are not corrected because there is no position feedback applied, and they can accumulate over time (as a cumulative lateral navigation error).

6.2 Lateral Navigation Methods and Errors

The predicted aircraft locations at the handshake times are affected by the allowed value for the lateral navigation error for the non-waypoint methods. Although this navigation uncertainty does not appear to be specified by the aircraft manufacturer, I can estimate a value based on the expected uncompensated crosswind fluctuations. The variable crosswinds disturb the aircraft track, and there is no position feedback (in the "non-waypoint" navigation modes) to compensate the lateral drift of the aircraft off the desired course. The mean crosswind is compensated when flying a constant track (by adjusting the heading), but variable crosswinds cause the actual aircraft path to wander left and right, depending on the crosswind fluctuations. As a rough approximation, consider a 3.5 knots RMS uncompensated crosswind fluctuation acting on an aircraft with an air speed of 450 knots. As a percentage of forward air speed, this is 3.5 / 450 = 0.78% of the forward speed, which is equivalent to a 0.45° track angle error. Therefore, a value near 1/2° appears consistent with several knots of uncompensated equivalent crosswind.

I first estimated the RMS value of the lateral navigation error as 1/3°, and this allowed the initial detection of the MH370 SIO Route signature. That value was then adjusted to 0.46° so the BTO residuals of the correct route would closely match the 29 μs estimate per DSTG [16]. The assumed lateral navigation error affects, in an inverse fashion, the best-fit CBTO residuals.

The formula for the normalized RMS lateral navigation error is:

$$(5)\quad \Sigma_{LatNav} \equiv \text{RMS(Lateral Navigation Residuals)} \;/\; 0.46^\circ .$$

The four lateral navigation methods not using waypoints, and therefore subject to these ≈ 0.46° RMS errors, are:

(1) Constant True Track (CTT),
(2) Constant Magnetic Track (CMT),
(3) Constant True Heading (CTH), and
(4) Constant Magnetic Heading (CMH).

It is also possible to insert a constant track or constant heading leg in the planned route using the FMC. It is not necessary to use the MCP for directional modes – the FMC is also capable of doing this [3].

For waypoint navigation using the FMC LNAV mode, the allowable lateral navigation errors from leg to leg along a route to a waypoint are essentially zero. In this case, the tracks must match a great circle (also called a geodesic).

6.3 Straight Versus Curved Routes

The differences between straight and curved autopiloted routes into the SIO are important in locating the aircraft debris field as well as in understanding how and possibly why the aircraft was put into a particular navigation mode. For example, LNAV to a waypoint requires a destination. CTT (and indeed all the MCP lateral navigation modes), is a directional command, not a destination command. So straight routes can be either directional (generally using the MCP, and in case of a FMC route error, the FMC itself) or to a destination (LNAV to a waypoint using the FMC).

In addition, directional commands from the MCP and from certain error modes in the FMC can produce autopiloted curved routes. Therefore, if the route were curved, generally it must have either been implemented using the MCP to set a flight direction, not a destination, or possibly an error occurred in the Active Routes page in the FMC because of incomplete route entry or failure of the pilot to remove a lateral offset before reaching a Holding fix.

There are three possible curved routes: Constant Magnetic Track (CMT), Constant True Heading (CTH), and Constant Magnetic Heading (CMH). Moving south from the equator into the SIO, lines of constant magnetic variation curve to the east (by about 15° in the case of MH370), so constant magnetic reference routes will produce flight paths that also curve eastward by about 15°. In addition, on this particular night, the high-altitude winds in the SIO were fairly strong from the west. These crosswinds will also push an aircraft flying a constant heading farther eastward as the aircraft flies generally southward. Thus, the CMH route has two curvature effects which both are in the same eastward direction (magnetic variation and crosswind), and this leads to extreme route curvature. It is so large, in fact, that this case is difficult to match to the Inmarsat data.

The FMC does, in certain situations, implement a directional lateral navigation mode when certain errors occur, such as a Route Discontinuity or an End of Route Error [3]. This can happen, for instance, if no waypoints are added past the one just reached. Also, an error occurs when a Holding fix is approached while a lateral offset is still active (and not removed by pilot action). Generally speaking, the default lateral navigation method used by the FMC in these cases is a constant heading mode, with the bearing reference being either true or magnetic, depending on the current setting of the NORM/TRUE switch located near the display units. Except at high latitudes near the poles, the NORM/TRUE switch is kept in the NORM position, which means that the reference for the

bearing is magnetic. Thus, a FMC error would be expected to result in a Constant Magnetic Heading command (i.e., CMH) and not a Constant True Heading command (i.e., a CTH route).

Another possibility is that the MCP was used to set a Constant Magnetic Track (CMT). This can be done in two ways. First, the TRK/HDG toggle switch on the MCP must be in the TRACK position. Then one can maintain the current Magnetic Track simply by pushing the TRK HLD (i.e., TRACK HOLD) switch. This method allows the entire range of bearings to be possible, not just integer degrees, but fractional degrees. A second method is to select a given track angle in whole degrees using the TRK SEL controls on the MCP followed by activation of TRK HLD to maintain that Magnetic Track angle. Of course, the NORM/TRUE switch must be also in the NORM position, which is expected when flying in this region of the world. For instance, if a pilot (or even a cabin crew member) wanted to fly due south, one could simply select 180° and hold that bearing, which would most likely be a magnetic reference (with the reference switch set to NORM). A CMT may also be commanded using the FMC, but it is simpler to implement using the MCP.

6.4 Degree of Rotational Symmetry in the Satellite Data

The high degree of rotational symmetry of the CBTO arcs allows a continuous band of approximate solutions, roughly one to several degrees wide in bearing, rather than one or several tightly-constrained bearings. In fact, if the satellite were stationary, the route bearing would be extremely difficult to determine because the CBFOs are not highly sensitive to true track at all bearings. In this MH370 case, the satellite moved during the flight, creating rotational asymmetry (i.e., the CBTO arcs do not have a common center), and this allows a specific solution for the route bearing. Of course, the satellite also contributes its own Doppler shift to the BFO parameter because of its speed toward or away from the aircraft.

In addition to the asymmetry of the satellite data caused by the motion of the satellite, the temperature and winds aloft varied with position, altitude, and time, providing additional and important rotational asymmetry in the data set and resulting in enhanced ability to discern the exact route bearing. Similarly, the magnetic variation is position-dependent, and this also creates rotational asymmetry in the satellite data, allowing a more specific solution for magnetic-reference routes.

7. Environmental Models

7.1 Along-track Wind Errors

I compute the predicted air speed using my air speed model which incorporates flight level, air temperature, and aircraft weight, plus a specified B777-200ER air speed control mode and setting. Therefore, candidate routes being fitted have a predicted ground speed that depends on the commanded air speed and the GDAS wind speed component in the “along-track” direction (which is similar to the tailwind, but in the track direction, not in the heading direction).

I must also allow for GDAS wind speed errors of up to 5.7 kts RMS [14] which affect the ground speed in the along-track direction for all lateral navigation methods (including LNAV via waypoints). This wind error effect is independent of both the lateral navigation method and the air speed control method used. Ignoring this critical wind error effect on ground speed can lead to false route fitting results or incorrect CBTO error estimates. In fact, the aircraft is incapable of flying at a constant true air speed, nor can it fly at a constant true ground speed. In normal ECON cruise, its Mach is adjusted by the FMC depending on aircraft weight and flight level. Its true air speed varies with weight, flight level, and air temperature. Its ground speed varies with weight, flight level, air temperature, along-track GDAS wind speed, and along-track GDAS wind speed error. In my Route Fitter, the length of each leg, calculated from the latitude/longitude positions of the end points, is also corrected for the additional path length due to leg curvature when present. This very slightly increases the calculated ground speed.

The along-track wind error is simply the difference between (a) the ground speed estimated by the vector sum of the air speed model prediction and the along-track wind speed, and (b) the ground speed calculated from the

range between the two end positions of each leg (i.e., the "handshake" positions). An example is shown in Figure 5.

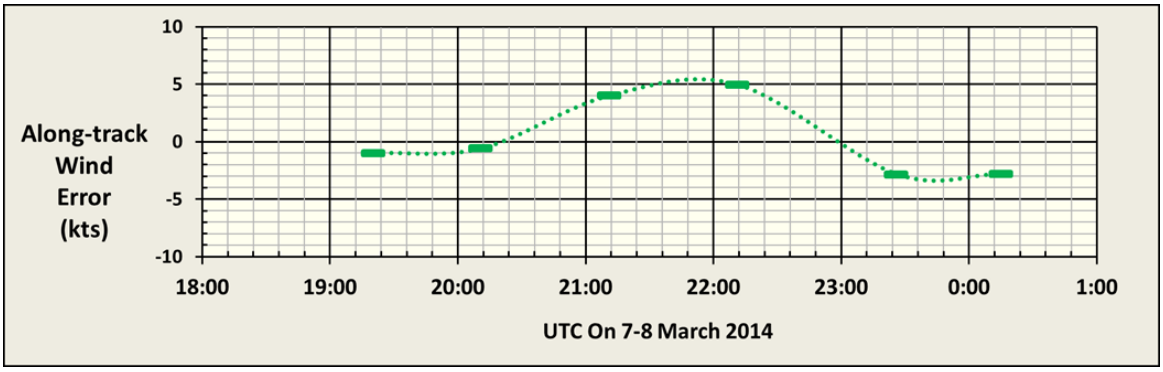

Figure 5. Typical Along-track Wind Speed Error for a SIO Route

In order to predict the aircraft ground speed, I model the aircraft weight, the air temperature, the wind speed, and the along-track wind speed error over a route (assumed to be at a constant flight level). This is quite a complex task since the temperature and the wind vary in four dimensions (latitude, longitude, flight level, and time). My route fitting program takes all these factors into account, and it interpolates the GDAS temperature and wind over the four dimensions at points along the route being fitted.

The 5.7 knot expected GDAS wind speed errors consider the entire globe, the entire atmosphere from sea level to stratosphere, and any specified time. I expect that, over a limited geographical range (i.e., the SIO), at a constant altitude, and over a 5-hour time period, the statistical wind error will be significantly smaller than 5.7 knots. In this paper I use 3.5 knots RMS for both the along-track and the cross-track wind errors. This is an approximation I made to a statistical quantity for which I have an upper bound (5.7 kts) and a lower bound (0 kts). The particular value of 3.5 kts was chosen so the MH370 SIO Route fit had a GOF very near 1.0, although this particular wind error value has no material impact on identifying that unique route.

Figure 6 illustrates the winds at FL340 over the SIO from the GDAS database at a time near the end of the MH370 flight [7]. The gold dot is waypoint BULVA, which is near the FMT. The green circle is my predicted 7th Arc location. Near BULVA the winds are fairly light and from the east. The winds decrease as one goes southward from BULVA, and then the winds increase significantly and blow from due west as one approaches the 7th Arc. Thus, the winds over the SIO on this night are primarily across the flight path, changing direction from the left side of the aircraft to the right side, and strengthening at the end of the flight. This has a significant effect on the curvature of constant-heading routes, blowing the aircraft first slightly to the west (due to wind from the east), and then more strongly to the east (due to wind from the west).

7.2 Cross-track Wind Errors

For the two constant-heading routes (magnetic and true), left cross-track wind errors (also assumed to be 3.5 kts RMS) must be added to the nominal GDAS cross-track winds. This is done in my SIO Route Fitter. In these two constant-heading cases, there are four crosswind errors that are synthesized for the four "legs" between the five handshake times from 19:41 and 00:11. These cross-track winds and cross-track wind errors cause changes in the true tracks of each leg along the route because they translate the aircraft in the cross-track direction during its flight (for the two heading modes only). Each leg has wind errors (both along-track and cross-track) that are assumed to be independent. The along-track errors are determined directly by subtracting the average ground speeds of each leg (found from the best-fit handshake locations) from the predicted ground speeds found using the air speed model and the GDAS along-track winds. For the heading modes only, the cross-track wind errors are four additional variables that are fitted during the route fitting process, generally for a total of 15 (10 latitudes and longitudes, speed setting (if needed), and the four cross-track wind errors).

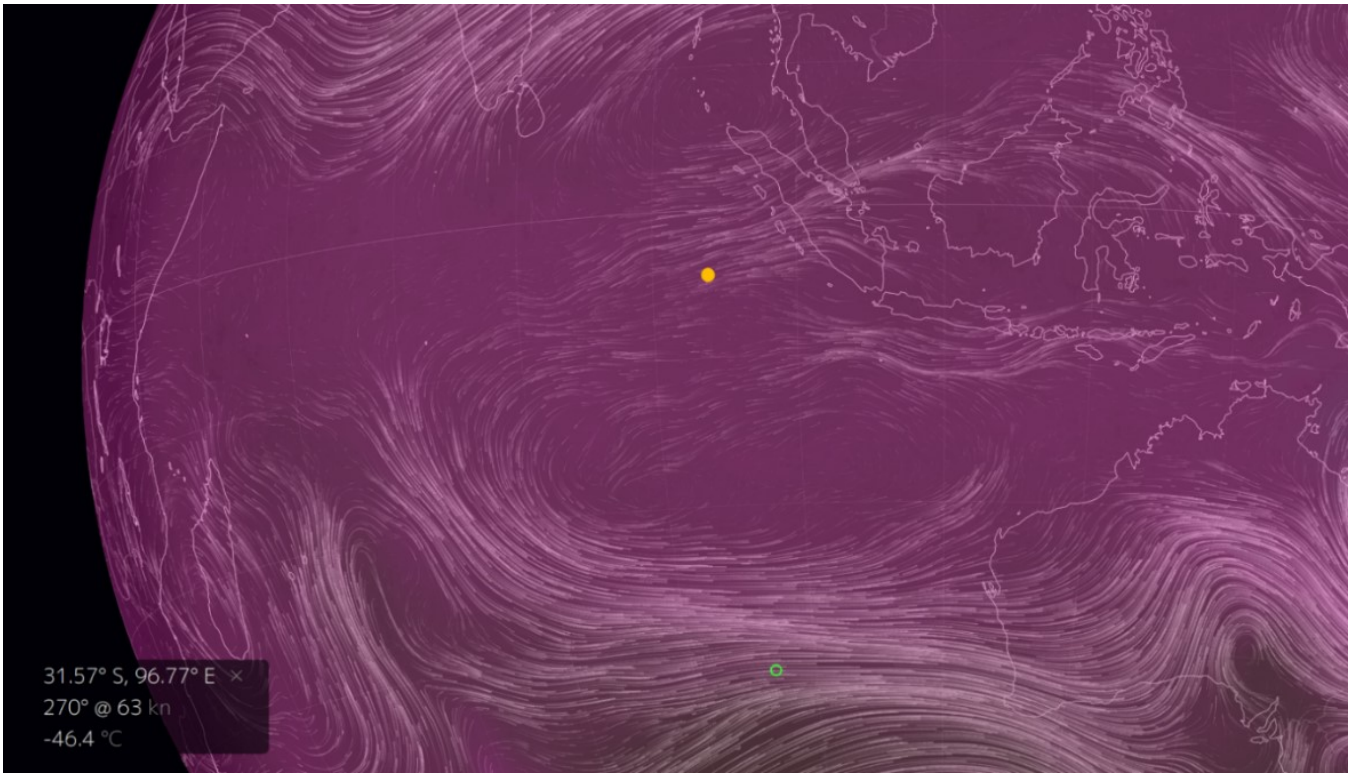

Figure 6. Winds Over SIO on 8 March 2014 at 00:00 UTC and at 250 hPa (FL340)

I hold the mean bearing fixed, so it becomes a condition on the latitude/longitude parameters, and it is not itself a fitted parameter. The air speed is dependent on the positions, so including it does not increase the number of independent variables. In addition, I am only constraining the RMS value for the cross-track wind errors, so this effectively adds only one independent variable, for a total of 11 independent variables.

For the "track" modes (CTT, LNAV using waypoints, and CMT), I solve for 10 or 11 variables (5 pairs of latitude/longitude and the speed setting, if needed) using the 5 pairs of CBTO/CBFO values at the handshake times from 19:41–00:11. In these cases, the speed is dependent on the handshake locations, so the number of independent fitted variables is 10, matching the data set.

7.3 Strong Variations of Temperature with Altitude and Latitude

Figure 7 shows the static air temperature (SAT) difference (Δ_{SAT}) from the International Standard Atmosphere temperature (i.e., $\Delta_{SAT} \equiv SAT - SAT_{ISA}$) for a SIO Route at FL335. It illustrates the actual temperature deviation profile with time for the flight level that MH370 may have experienced. The decline at 00:11 is due to 9M-MRO descending after fuel exhaustion.

Of course, the temperature profile along the flight path affects the true air speed, as well as the fuel flow. So, I must have a 4-D temperature model (which varies with latitude, longitude, pressure altitude, and time). This information is provided by the NOAA GDAS database [7] [8]. I interpolate each predicted location in latitude, longitude, pressure altitude, and time to obtain air temperature (and wind speed and direction). The temperature variations from the standard atmospheric conditions are large for MH370, especially so as a function of altitude. One must use the GDAS data set in order to have accurate predictions for air speed, ground speed, and fuel consumption in modeling MH370. In particular, the temperature deviation for standard ISA conditions varies significantly with altitude, and this strongly affects both the fuel mileage and the endurance.

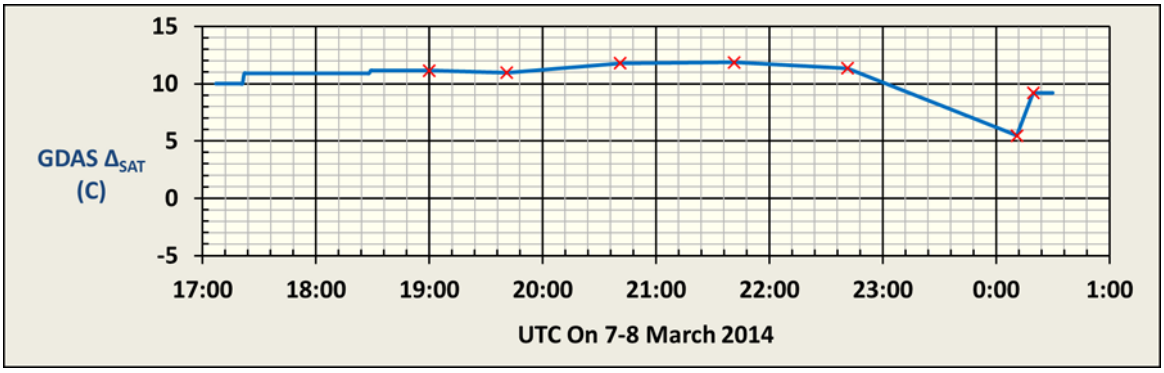

Figure 7. Example of Static Air Temperature Deviation from the ISA SAT Along a Route

Previously, I predicted the altitudes to match MEFE for various speed modes assuming that Δ_{SAT} = +10C at all altitudes [12, 13, 11]. Now I use a full 4-D GDAS database of wind and temperature data for this purpose [8]. It reveals large differences in Δ_{SAT} with altitude and latitude. Some examples of the GDAS air temperature variation with altitude, at different locations and times, are shown in Figure 8 and in Figure 9.

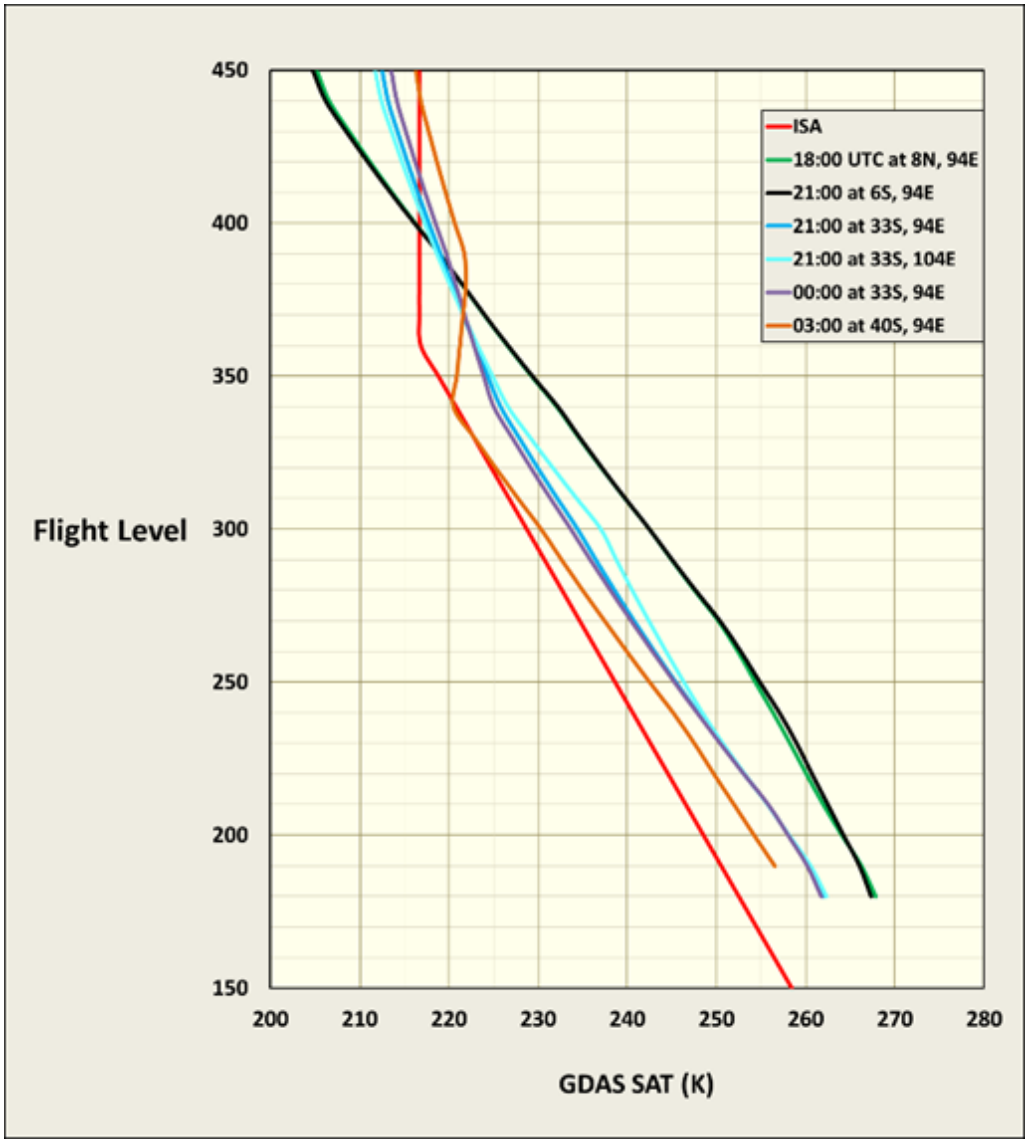

Figure 8. Static Air Temperature Profiles for 7 March 2014

In Figure 8 the green line is the region and time most closely corresponding to the FMT (roughly 18:00 UTC near 8°N, 94°E). The black line is for a time 3 hours later at 21:00 UTC near 6°S, 94°E. These two profiles are virtually identical. This result implies the region within about 10° of the equator is quite stable, although the "knee" in the red curve (the boundary between the troposphere and the stratosphere) in the ISA profile near FL360 is shifted up to FL440.

The blue, turquoise, and purple curves in Figure 8 are nearly identical, demonstrating that the variations with longitude and with time near 33°S are almost nil. The strongest temperature dependence at a given altitude is on latitude once south of the equatorial zone. As one goes further south into the SIO, the air gets colder, the tropopause is lower, the true air speed is lower, and the engine fuel flow is lower.

The temperature deviations from ISA are from -10C to +15C in Figure 8. This has a pronounced effect on fuel consumption because fuel flow increases by 1 % for roughly every 3C of increase in Δ_{SAT}. Since the "book values" of fuel consumption are for ISA temperature (the red line in Figure 8), the actual fuel consumption of MH370 varied with the atmospheric temperatures encountered. This effect is included in my fuel flow model and is taken into account in finding the optimum speed/altitude combinations to match MEFE.

Figure 9 provides some additional examples of vertical GDAS temperature profiles

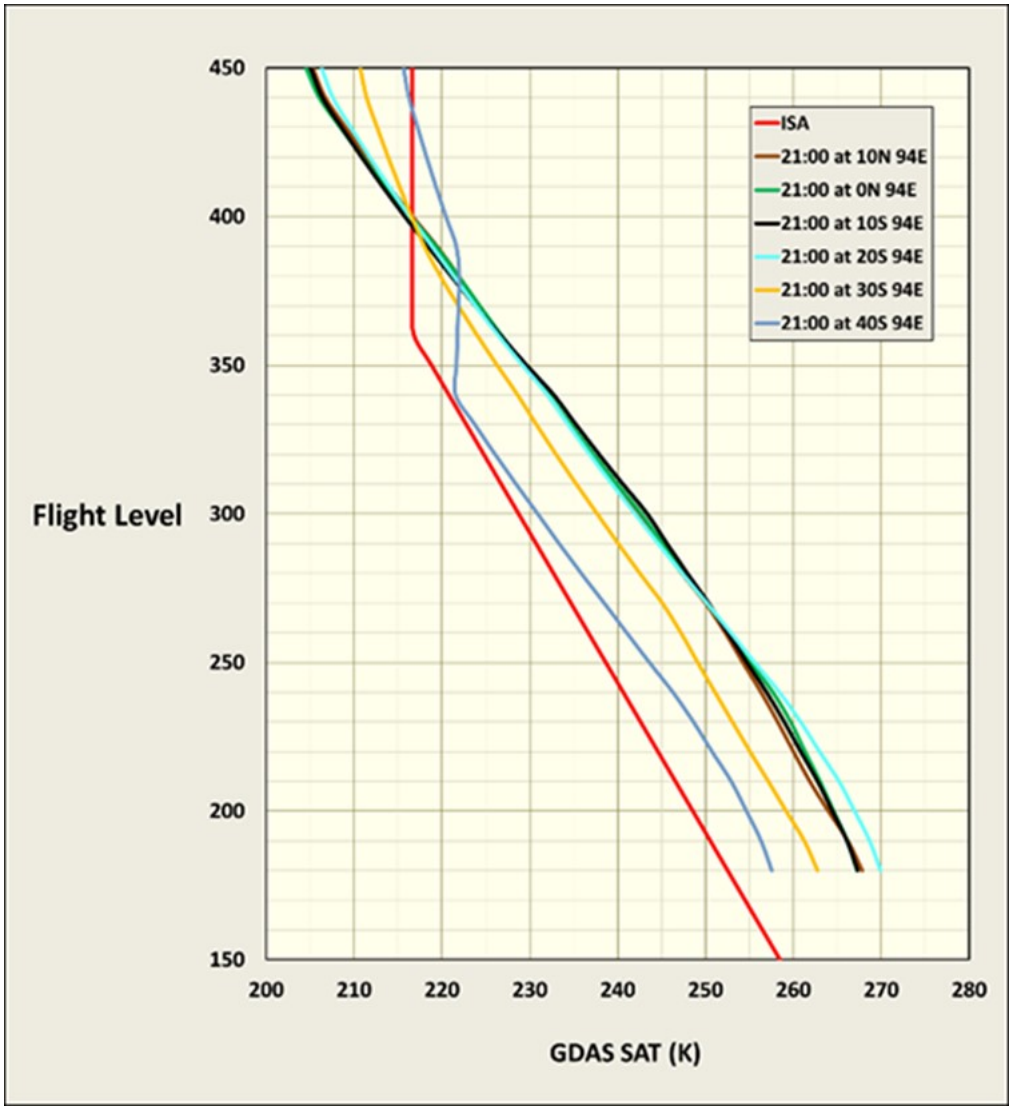

Figure 9. More Static Air Temperature Profiles for 7 March 2014

Figure 9 shows the invariance with time and with latitude within 10° of the equator and the strong latitude dependence below FL390, which is reduced to nearly no change at FL400 from the equator down to near 40°S. Below FL400, as one goes further south, the air gets colder, the true air speed gets slower, and the fuel flow is lower.

Between the handshake times, I do a linear interpolation of temperature, as illustrated previously in Figure 7. I vector average the winds at the start and the end of each route leg when computing the average leg along-track wind speeds.

The True Air Speed (TAS) declines with time during the SIO route for two reasons: (a) the temperature is falling at greater distance from the equator, so a constant Mach results in a declining KTAS in colder air, and (2) in ECON mode (such as Maximum Range Cruise, which is ECON with Cost Index = 0), the FMC decreases the Mach number as the aircraft weight declines due to fuel being consumed. Together, these two effects result in a significant drop in KTAS of about 25 kts from 19:00 to 00:00 UTC for Maximum Range Cruise.

8. Route Fitting

8.1 Overfitting Can Lead to Route Parameter Contamination by Data Noise

Note that GOF = 0 means that the route model was able to fit exactly each of the 10 satellite data points used to search for the MH370 route (i.e., all the residual errors are zero). This obviously would be a case of overfitting the data with an overly complex route model which has an excessive number of degrees of freedom. The result is not meaningful because it assumes the actual noise in the data represents real and significant course changes, which it does not. Route fits with very small residuals and a small GOF value cannot be the correct route. Because of the route model, assumptions, and conditions I use in my route fits, such a false result is not possible in this analysis.

8.2 Route Fitting Process

I have modified my route fitting process to allow faster optimization. It is important in this regard to make each fitted handshake location as independent as possible from the other locations. Otherwise, creating a trial route requires integrating a piece-wise linear connection of short movements, and adjustments in any handshake location therefore necessarily affect all of the later fitting errors. That method substantially increases the computer run time to converge on a route solution compared to directly optimizing the (independent) coordinates of each handshake location along the route, which is what I do in my Route Fitter.

In addition, instead of directly comparing the air speed of a trial route to an air speed model, I now do the comparison using the ground speed parameter. The advantage of this method is substantial because the ground speed can be found directly from the fitted latitudes and longitudes of the handshake locations, without any knowledge of wind or temperature or flight level or speed control mode. Those parameters all affect a prediction model of ground speed, which begins with the air speed model (which depends on the speed control mode, speed setting, flight level, and air temperature). Then I vector sum the along-track wind speed to determine the model ground speed. Finally, the difference between the two ground speed estimates, one from the best-fit latitudes and longitudes, and the other from the air speed model and the temperature/wind data, is the wind error in the track direction. For constant-heading navigation modes, the (left) cross-track wind errors are fitted to minimize the lateral navigation errors.

8.3 Route Fitter

The program I use for optimizing route parameters comprises 68 worksheets in a 72 MB macro-enabled EXCEL .xlsm file. Each worksheet is a process model, an environmental database, a satellite database, or an aircraft database. The main program is called the Route Fitter. It contains the lateral navigation equations for each of the possible methods. It calls each of the process model or database worksheets as needed to obtain environmental

data (wind, temperature, and magnetic variation), aircraft data and predicted parameters, satellite data, and waypoint positions. The Route Fitter also contains the route fitting metrics, the Optimization Function, and a vector table containing the results of 200 saved trial runs. Each trial run of the Route Fitter, given a fixed mean initial bearing, required about ½ to 1 hour on a high-speed business laptop computer running Microsoft Windows 10 and Excel 2016. In most cases, multiple trial runs were done with slightly modified constraints. The total computing time of the results presented here is approximately 400 hours.

8.4 Route Fitting Strategy

The general approach is to search, for each of the five lateral navigation methods, at 1° intervals in bearing until a region of interest is detected where there is a general minimum in the Goodness of Fit metric. Next, the air speed mode and setting are selected to optimize the fit. Then, a fine-scale mapping of the region of interest at ≈ 0.1° intervals is done, looking for a central peak within the region of interest. If found, this feature indicates the MH370 SIO Route.

8.5 Matched-filter Detection

Within a region of interest, this route search process is a matched-filter maximization. The output of the matched filter is the Goodness of Fit metric. It is maximized, within the region of interest, at the central peak. Thus, a local maximum in the Goodness of Fit, with a value near 1.0, identifies the route because the satellite data is well-matched by the predicted CBTOs and CBFOs of the synthesized route.

8.6 Objective Function

The choice of an Objective Function to be minimized in the route fitting process is critical. My Objective Function, which is minimized by the Route Fitter, is the RMS combination of the Goodness of Fit metric (which depends on the RMS values of the 5 CBTO residuals and the 5 CBFO residuals), and three additional, simultaneous conditions:

(1) The along-track wind speed error is held at 3.5 kts RMS, within < 1%.
(2) For the Heading modes, the left cross-track wind error is also held at 3.5 kts RMS, within < 1 %.
(3) For the four “directional” lateral navigation modes (CTT/CMT/CTH/CMH), the RMS of the four leg track errors is held at 0.46°, within < 1 %.

The addition of these simultaneous conditions produces different best-fit route parameters and CBTO/CBFO noise statistics than when simply minimizing the Goodness of Fit metric. That difference is what makes it possible to identify the MH370 SIO route. This happens because the CBTO and CBFO noise statistics are not always minimized by this Objective Function; at the correct route they rise above their minima to their true values. This only occurs when there is effective separation of the systematic route contribution and the random noise in the CBTO/CBFO data, and this only occurs at the correct route.

The weighting factors of the terms in the Objective Function must be monotonic for nonlinear optimization algorithms to work effectively (I use SOLVER in Microsoft EXCEL). I make the weighting factors a function of the magnitude of the normalized parameter error (= ”MNPE”). When the MNPE is > 1, the weighting factor is proportional to the MNPE. This provides heavy weighting on the (square of the) parameter which has the highest error. When the MNPE is < 1, I use a high power (= 6) of MNPE for the weighting factor. Thus, the weighting factor is highly nonlinear below unity MNPE. This creates a “cliff” at ≈ 90% MNPE, so that smaller errors contribute almost no constraint to the solution, but MNPEs near 1 and higher are significantly (and increasingly) weighted. The result is that all parameters tend to converge to the same normalized error magnitude (as good as the data and model allow) if there are sufficient degrees of freedom available in the route model to fully adjust each parameter.

8.7 19:00 Back-track Position

I also compute a "back-track" position (at a somewhat arbitrary time of 19:00) as an aid in connecting the 18:22-19:41 "FMT" route to the SIO route from 19:41–00:19. The back-track position is fitted by best satisfying these two conditions:

(1) the course is extended backward in time from the 19:41 position, following the desired course within 0.02 degrees, and
(2) the ground speed used is within 2 kts of the vector sum of the air speed model plus the along-track wind.

Note that the FMT may have occurred after 19:00 (but certainly before 19:41), so the aircraft may not actually have overflown the 19:00 "back-track" position. Still, it provides a useful track for comparison with the aircraft path through 18:28 plus nearby waypoints, in order to understand the range of maneuvers that must have occurred between 18:29 and 19:41 that led to the SIO Route.

8.8 00:19:37 Position

The 00:19 data are not used for primary route fitting because fuel exhaustion in the right engine occurred near 00:11, and this reduced the speed after 00:11. In addition, when the left engine also failed at 00:17:30, a bank developed and the course most likely changed by 00:19 in a way that is not predictable. Therefore, it is unwise to use the 00:19 Inmarsat CBTOs and CBFOs for the primary route fitting. The CBTO at 00:19:37 is useful in determining the most likely intersection of a continuation of the flight path with the 7th Arc, and this is done in a separate fit after the 19:41-00:11 route is determined.

In order to find the 00:19:37 position (i.e., the 7th Arc latitude and longitude), I fit the additional leg from 00:11 to 00:19:37 subject to the following three desired conditions:

(1) the ground speed error is less than 10 kts,
(2) the CBTO error is < 2 μs, and
(3) the track error is < 2° from the nominal route.

Thus, generally speaking, the 00:19:39 position is directly on the 7th Arc and is very close to a simple continuation of the current route (either straight or curved). The ground speed error from the 6th Arc (at 00:11) to the 7th Arc (at 00:19) is generally less than 10 knots when using my end-of-flight model to determine the average groundspeed. This is significantly slower than the speed during the previous legs due to fuel exhaustion and subsequent aircraft slow-down during this last leg from 00:11-00:19.

8.9 00:19:37 Rate of Descent

The Rate of Descent (ROD) is fitted to reduce the BFO error at 00:19:37 to < 1 Hz. Typically, this is near 15,000 fpm.

8.10 Fitting the Known Endurance

There is another condition that must also be matched – the endurance. That is given by the known MEFE time (estimated to be 00:17:30 on 8 March 2014 [10]). I use my fuel flow model and my endurance model to compute the fuel flows every minute from 17:06:43 (i.e., the time of the last MH370 ACARS fuel report [24]) until MEFE occurs. For each route fit, I adjust the average engine PDA so that MEFE is predicted to occur at 00:17:30 ± ½ minute. The PDA must match the known value for 9M-MRO (1.5%, [15]) within the fuel flow model error, which is estimated to be ± 2% (2σ) [11]. The choice of air speed control mode, speed setting, flight level, air temperature, and PDA all affect the predicted MEFE time. Thus, I do some iterative optimization of air speed control mode, speed setting, and flight level to match the MEFE time and provide a good fit to the BTO/BFO data, while also matching the PDA within the expected bounds (1.5% ± 2.0%).

9. Route Search

The MH370 SIO Route may be identified using multiple route fits to the satellite data, as illustrated in Figure 10.

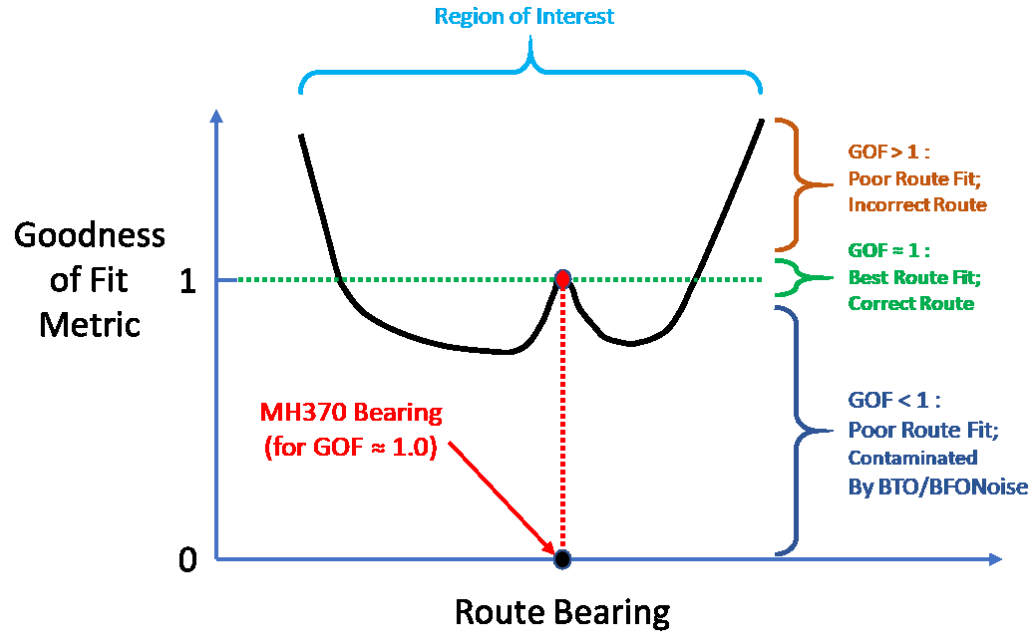

Figure 10. Expected Behavior of the Goodness of Fit Metric

Figure 10 shows the expected variation in the Goodness of Fit metric with the most critical route parameter – the bearing. Figure 10 is a plot of the Goodness of Fit result when the 10 latitude/longitudes are computed from the 10 CBTOs/CBFOs from 19:41–00:11 at fixed values of the route bearing. That process is what the Route Fitter does. It starts with 5 CBTOs and 5 CBFOs at 5 known (handshake) times, and it computes the CBTOs and CBFOs for a synthesized route, defined by 5 latitude/longitude positions. The route parameters are varied until the residual differences (i.e., residual errors) between the input CBTOs/CBFOs and the predicted CBTOs/CBFOs for the synthetic route are optimized (not minimized) by minimizing an Objective Function that includes three additional conditions.

The most critical route parameter is the initial bearing. The initial bearing does not change during the route for the constant-track and constant-heading routes, but the bearing does change slowly for the waypoint-to-waypoint great-circle routes using LNAV. In that case the initial bearing for each leg is calculable, and it is equal to the final bearing of the preceding leg.

The (initial) bearing at 19:41 is used for the horizontal axis in Figure 10. The process to generate a curve like Figure 10 is simple in theory, but it is quite tedious in practice. First, I pick a lateral navigation method. Then I choose a value for the bearing (in degrees). Next I optimize the fit by minimizing an Objective Function while varying all the other route parameters (i.e., all but the bearing). The Objective Function in the Route Fitter is a modified version of the Goodness of Fit that incorporates the three additional necessary conditions. Then I repeat the process to map out the GOFs for a wide range of bearings. I get curves similar to the black line in Figure 10.

This signal processing method is equivalent to passing a matched filter over the data set. The filter in this case is operating on the CBTO/CBFO data set. It attempts to correlate the contributions from each data point by summing them with a weighting pattern (i.e., a route) that is very high-Q and multi-dimensional. The output of the matched filter is the Goodness of Fit metric. The weighting pattern is the model predictions of CBTO/CBFO for a particular set of route parameters. When those parameters "match" the data set, the filter has an increased output compared to the local neighborhood. A peak in the output indicates a detection – in this case a match with the

correct route. When the match is complete, the Goodness of Fit will have a value of unity as shown by the central peak in Figure 10.

9.1 Impact of Noise in the CBTOs and CBFOs

When the GOF is significantly less than 1, the fit is poor because the route parameters are being excessively fitted to the data noise. The residual fitting errors are too small, and they do not match their expected RMS values. This case is the region well below the GOF = 1 line shown in Figure 10, where the route parameters are contaminated by the noise in the data.

There are three noise statistics affecting the dispersion of the fitted CBTO residuals:

(1) the CBTO noise itself (29 μs RMS),
(2) the along-track wind errors (≈ 3.5 knots RMS), and
(3) the lateral navigation errors (≈ 0.46° RMS for the non-LNAV modes).

The last two of these statistics are not precisely known, and other nearby values could be used instead, so long as their combined effect is similar. That is, if one allowable value of a statistic is increased, the allowable value of the other statistic must be decreased in order to maintain the known 29 μs RMS CBTO noise for the correct route. So, similar results may be obtained with somewhat higher along-track wind errors and somewhat lower lateral navigation errors. It is not necessary to determine their exact values in order to identify the MH370 SIO Route. Reasonable approximations of these two parameters are adequate for this purpose.

9.2 Impact of Systematic Route Errors

When the fitted route does not closely match the actual MH370 route, systematic errors exist, and these generally increase the CBTO/CBFO RMS normalized errors well above 1.0. In this case, the overall GOF is also greater than 1.0. When the GOF is significantly > 1, the fitted route cannot be the MH370 route. Therefore, a fit with GOF $\gg$ 1 demonstrates that this particular route was not flown by MH370. This is the region well above the GOF = 1 line in Figure 10.

9.3 Identification of MH370 Route

The "correct" MH370 Route may be identified as the unique feature whose shape is similar to that shown in Figure 10 at the bearing labeled "MH370 Bearing". This feature in the plot of GOF versus bearing must have the following characteristics:

(1) It has a peak GOF value very near 1.0.
(2) Both of the normalized BTO and BFO errors should be < ≈ 1.2.
(3) The GOF feature is narrow in width, being roughly equal to the RMS lateral navigation error.
(4) The "central peak" is surrounded by substantially lower GOF values at both larger and smaller bearings.
(5) There is only one such peak among all the methods of lateral navigation.

If no peak is found, then whatever particular route variant is being studied was not used by MH370. This peak must be present at, and only at, the correct route bearing with the correct lateral navigation method and at the correct speed.

9.4 Route Search Strategy

Curves similar to Figure 10 were generated for each lateral navigation method: CTT, LNAV, CMT, CTH, and CMH. If only one GOF peak feature is found, that peak is the "digital signature" of the correct MH370 route. The intersection of that route with the 00:19:37 Arc is therefore the best predictor of the location of the debris field from aircraft 9M-MRO.

For each lateral navigation method, I evaluated each speed control mode, varying the flight level and the PDA so as to obtain the best GOF subject to maintaining the predicted MEFE at 00:17 with a PDA within 2% of 1.5%. The results of this optimization are shown in Table 2, which identifies the combinations of flight level and air speed control mode that were possibly used for each lateral navigation method.

Table 2. Air Speed Optimization Results

Lateral Navigation Method	Speed Control		Flight Level	PDA	MEFE	Average from 19:41-00:11			Σ_{CBTO}	Σ_{CBFO}	Best Goodness of Fit	Bearing for GOF < 1.2		00:19:37 Location	
	Mode	Setting				Δ_{SAT}	TAS	Bearing				Min	Max	Latitude	Longitude
		(Mach or KIAS)	(hft)	(%)	(hh:mm)	(C)	(kts)	(°)	(---)	(---)	(---)	(°)		(°)	
CTT	LRC		398	1.0%	00:17	0.7	482.5	183.0	0.75	1.03	0.90			-35.82	91.77
	Econ CI=52		400	2.6%	00:17	0.2	475.3	183.0	0.70	0.99	0.86	182.2	183.6	-35.83	91.76
	MRC		401	3.5%	00:17	0.1	470.8	183.0	1.25	0.96	1.12			-35.76	91.85
	HOLDING		417	3.5%	00:17	-3.5	467.6	183.0	1.02	0.89	0.96			-35.75	91.86
	KIAS	250.0	405	2.5%	00:17	-0.9	476.7	183.0	0.89	0.93	0.91			-35.79	91.80
	MACH	0.820	389	2.8%	00:17	3.0	473.4	183.0	0.92	0.92	0.92			-35.78	91.83
LNAV (Waypoints)	LRC		379	-0.5%	00:17	4.9	485.2	182.0	1.92	1.13	1.58			-35.45	92.28
	Econ CI=52		382	1.5%	00:17	4.4	478.3	182.0	2.42	1.05	1.87			-35.55	92.16
	MRC		388	3.0%	00:17	3.2	472.1	182.0	2.58	0.97	1.95			-35.42	92.32
	HOLDING		No solution (no PDA within range matches MEFE at accessible altitude)											---	---
	KIAS	255.1	400	1.4%	00:17	0.3	481.4	182.0	1.83	1.11	1.51			-35.52	92.20
	MACH	0.840	400	0.8%	00:17	0.3	481.8	182.0	1.77	1.10	1.48	---	---	-35.52	92.20
CMT	LRC		375	-0.5%	00:17	5.6	484.5	181.6	10.77	1.26	7.66			-32.69	95.67
	Econ CI=52		344	-0.5%	00:17	9.8	465.8	181.6	5.93	1.18	4.28			-32.27	96.10
	MRC		336	2.7%	00:17	10.3	443.2	181.2	1.00	1.00	1.00	180.2	182.1	-31.57	96.77
	HOLDING		No solution (no PDA within range matches MEFE at accessible altitude)											---	---
	KIAS	260.6	343	2.9%	00:17	10.0	448.7	181.2	2.05	0.99	1.61			-31.62	96.72
	MACH	0.757	340	2.5%	00:17	10.1	448.9	181.2	2.06	0.99	1.62			-31.63	96.72
CTH	LRC		374	-0.5%	00:17	6.1	484.7	177.4	6.96	1.31	5.01			-32.00	96.25
	Econ CI=52		338	-0.5%	00:17	10.2	463.1	177.4	2.15	1.20	1.74			-32.22	96.12
	MRC		344	2.4%	00:17	9.9	450.1	177.4	1.92	1.07	1.55	---	---	-31.90	96.44
	HOLDING		No solution (no PDA within range matches MEFE at accessible altitude)											---	---
	KIAS	258.0	357	3.2%	00:17	9.3	454.2	177.4	3.69	1.07	2.72			-32.17	96.18
	MACH	0.765	343	2.5%	00:17	9.9	452.3	177.3	2.49	1.02	1.90			-31.93	96.39
CMH	LRC		No solution (no PDA within range matches MEFE at accessible altitude)											---	---
	Econ CI=52		No solution (no PDA within range matches MEFE at accessible altitude)											---	---
	MRC		307	3.4%	00:18	12.3	422.5	178.0	1.87	0.95	1.48	---	---	-30.32	97.95
	HOLDING		No solution (no PDA within range matches MEFE at accessible altitude)											---	---
	KIAS	268.8	299	1.4%	00:17	12.8	432.7	178.0	3.97	0.88	2.87			-30.69	97.63
	MACH	0.714	306	2.4%	00:17	12.4	431.0	178.0	4.14	0.89	2.99			-30.66	97.66

A more detailed bearing curve was then generated, similar to Figure 10, for each lateral navigation method, using the best speed mode and altitude identified in Table 2.

9.4.1 *CTT Speed and Altitude*

The uppermost row of yellow cells in Table 2 is the best CTT result (i.e., with the smallest GOF), which is ECON with Cost Index = 52 (i.e., the Flight Plan) at FL400. This is quite a high altitude for the aircraft weight circa 19:41,

although achievable. MRC at FL401 was nearly as good as ECON with Cost Index = 52 at this altitude. The other speed control modes were not as good at matching the required speed profile.

For CTT routes, there are several speed control options which produce minimum GOFs < 1, since there is some tolerance of a few knots in True Air Speed that can be acceptable (recall the along-track wind errors are 3.5 kts RMS). By adjusting the altitude, multiple speed control modes can produce nearly equal TAS and ground speeds. Of course, one must also match the known fuel endurance, but, not surprisingly, this is also possible, as demonstrated in Table 2. As shown previously, the Static Air Temperature (SAT), relative to the ISA standard temperature, happened to vary significantly with altitude during the MH370 flight. In fact, near the FMT the actual SAT was +10C above the ISA SAT near Flight Level 340 (FL340). At much higher altitude, say near FL420, the difference was -5C. Since the fuel flow (relative to the Boeing tables) depends on this Δ_{SAT} temperature difference (or, more accurately, on the difference in Total Air Temperature, or TAT) by roughly 3.4% / 10C, then a 15C relative temperature difference changes the relative fuel flows (and the endurance from 17:07) by about 5%.

9.4.2 *LNAV Speed and Altitude*

Table 2 shows the best LNAV/waypoint result (in the second row of yellow cells), which is M0.84 at FL400. The best GOF for LNAV is too high (1.48) for this method to be a viable candidate for the MH370 SIO Route.

9.4.3 *CMT Speed and Altitude*

The row of green cells in Table 2 is the best CMT result, which is Maximum Range Cruise (i.e., ECON with Cost Index = 0) at FL336. In this unique case, GOF = 1. Note that, at this fairly low cruising altitude of FL336, there is a significant difference in true air speed between MRC (Cost Index = 0) and the Flight Plan (Cost Index = 52). Thus, for CMT, all speed modes other than MRC were judged to be unacceptable because their minimum GOFs were all > 1.5. In other words, for CMT navigation, only MRC can fit the satellite data very well. None of the other standard speed modes matched the satellite data using this lateral navigation mode.

For the CMT case, which contains the identified MH370 SIO Route, the speed/altitude for which GOF < 1 in the region of interest was used, and this combination also worked well on the central peak where GOF = 1. For the other lateral navigation modes, the bearing of the minimum GOF was chosen for the detailed bearing study, since that will maximize the probability that the correct route might be adjacent.

9.4.4 *CTH Speed and Altitude*

The third row of yellow cells in Table 2 is the best CTH result, which is MRC at FL344. This is nearly the same as the best CMT speed mode, but the GOF for CTH is much higher (1.55), so CTH is not the ideal fit.

9.4.5 *CMH Speed and Altitude*

The bottom row of yellow cells in Table 2 is the best CMH result, which is MRC at FL307. Its GOF is 1.48, so CMH doesn't match very well.

10. Identification of MH370 Route

Figure 11 shows the results of the new analysis method for the five lateral navigation methods. Each figure covers a region of interest identified by computing the Goodness of Fit over a very wide range of bearings. Within this region of interest, the fitting residuals are small enough to warrant being explored in detail. In each graph, the blue curves are the normalized CBFO residual errors (= ΣCBFO) as a function of the mean route bearing. The black curves are the residuals for the CBTO errors (= ΣCBTO), and the red curves are the overall Goodness of Fit (i.e., GOF = the RMS of the normalized CBTO and CBFO residuals). The horizontal green dashed line is for a constant value of 1.0, which represents an ideal fit.

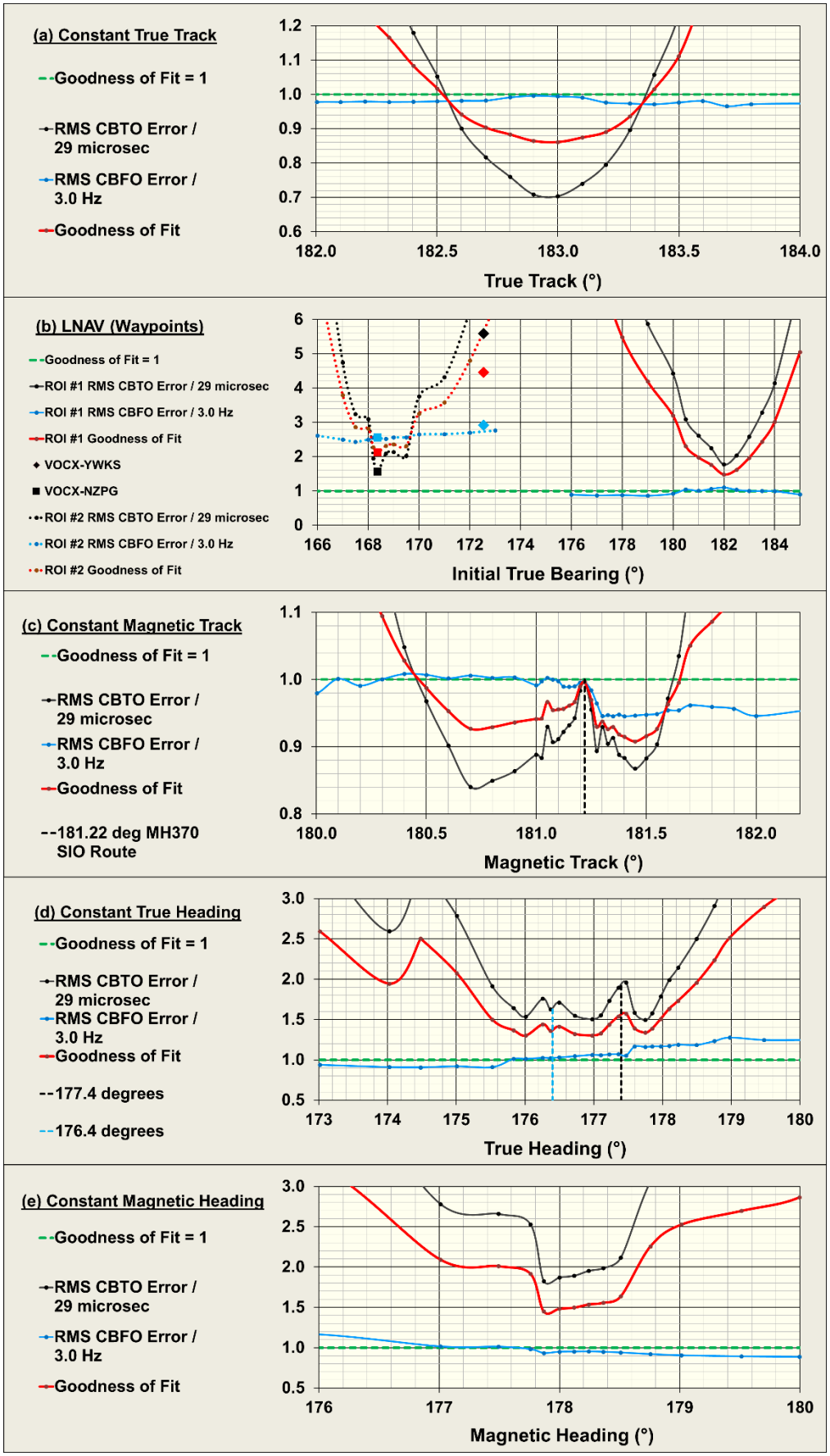

Figure 11. Figures of Merit for Five Lateral Navigation Methods

Comparing the expected shape for the GOF, shown in Figure 10, with the five curves in Figure 11, one can immediately see that only Constant Magnetic Track (CMT) has such a central peak feature at 1.0 GOF, and only at 181.22°. Constant True Heading has two weak peaks with GOF >1.7 that provide additional insight into the effectiveness of this route search method. They will be discussed later in this paper.

The new search strategy used in this paper requires both the CBTO and CBFO residuals to match their known RMS values, not that they be minimized. In addition, nearby bearings on both sides must have lower overall (i.e., Goodness of Fit) RMS values. This constraint applies mainly to the CBTO residuals, since the CBFO residuals vary slowly with bearing. The CBTO residuals will be locally maximized at the true bearing because the best-fit route parameters there are not contaminated by noise. Thus, I expect that the CBTO residuals will show a larger change in amplitude than do the CBFO residuals. In addition, the CBTO residuals will be larger at the correct bearing, but the CBFO residuals will show generally a smaller change. Finally, and very importantly, the bearing is not allowed to vary in any given fit. Instead, it is set to a fixed value, and it is changed incrementally from one trial fit to another.

10.1 Constant True Track Results

Figure 11(a) shows the CTT results. I searched the entire range of possible bearings to locate regions of interest where the residuals were at a minimum. This only occurred near 183° true track, and the region of interest there is narrow, being only about 1° wide. The CBFO errors are near 1, which is good, and the CBTO errors are less than 1 near 183°. However, the "central peak" feature is missing. Therefore, the MH370 SIO Route was not a Constant True Track.

10.2 LNAV Results Using Waypoints

Figure 11(b) shows the LVAV/waypoint method is similar in results to the CTT method. A primary region of interest was found; it is shown on the right side of the figure. It is about 1° wide, in this case near 182°, with a speed of M0.84 at FL400. Here the CBFO errors are good, being close to 1. However, the CBTO errors are never acceptable, having a minimum of 1.8. In addition, there is no central peak feature.

There is a second region of interest near 168° using M0.80 at FL350. This is plotted on the left side of Figure 11(b) as the dashed lines. Its minimum figure of merit is slightly worse than the high-speed 182° minimum, and neither is acceptable.

10.2.1 *Car Nicobar (VOCX) to McMurdo Station (NZPG)*

Iannello and Godfrey have proposed a LNAV waypoint route from the vicinity of Car Nicobar Air Force Base (VOCX) to Pegasus Field at McMurdo Station, Antarctica (NZPG) [25]. They allowed different, and generally more relaxed, acceptance tolerances on the fitting residuals than I have used in this paper, especially in the CBFO residuals, where they allow ≈ 7 Hz RMS. I compared my Route Fitter residuals, using their coordinates, with their reported results, and the CBFO errors matched within 1 Hz. Their RMS CBFO error was 8.1 Hz and my value was 7.7 Hz. Their CBTO error was 41 μs, and my value was 43 μs. That is excellent agreement considering the two fitting programs were independently developed. I show 2.5 kts RMS ground speed error using their handshake positions at the best speed I found (M0.798, which matches their value). That implies our temperature and/or wind predictions are slightly different, because Iannello and Godfrey did not allow for wind error at all. I expect some differences, because Iannello and Godfrey used only the environmental data at 00:00 UTC, whereas I interpolated according to the time along the route. However, the 2.5 kts difference is only a 0.5% RMS speed difference, so the agreement in calculated ground speed is good. My results for their route, using the same methodology as I used for the other routes reported in this paper, are shown in Figure 11(b) as the square symbols at 168.37° initial bearing. With 3.5 kts RMS along-track wind error allowed, I find the RMS CBTO error is 41 μs, and the RMS CBFO error is 7.8 Hz. The GOF is 2.10. As a result of my fitting requirements being more discriminating, especially with

respect to the CBFO residuals, I did not find their route to be acceptable as a candidate for the MH370 SIO Route. The NZPG route is not even the best LNAV route, and, so far, no LNAV route has either CBTO or CBFO fitting residuals small enough to be a viable candidate for the MH370 SIO Route (using my selection criteria).

10.2.2 *Car Nicobar (VOCX) to Wilkins Runway (YWKS)*

Godfrey [26] has proposed another LNAV waypoint route to Antarctica, this time to Wilkins Runway (YWKS). I have also analyzed that route using my Route Fitter, and the results are shown as the diamond symbols in Figure 11(b) at 172.55° initial bearing. Again, this route is far from meeting my acceptance criteria. It is not possible to achieve the 502 kts TAS Godfrey used, and the closest for a B777-200ER aircraft is 499 kts with M0.84 at FL338. At that speed, the YWKS route has 8.7 Hz RMS CBFO errors, 162 μs RMS CBTO errors, and a GOF = 4.5. At that speed and altitude, the fuel would be exhausted at about 23:35, 42 minutes before the established MEFE time. The fuel savings for a descent to FL200 before 18:40 and a Hold there, followed by a climb back to FL350 is < 1%, and this would only add 4 minutes of additional endurance. Even with the air packs turned off (a 2.5% fuel flow reduction) as well, the endurance shortfall for this route is still 28 minutes. Therefore, this route is not flyable by 9M-MRO. Thus, there are two reasons this route cannot be the MH370 SIO Route. It is not flyable with the fuel on board, and the fitting residuals are very large, as shown by the diamond symbols in Figure 11(b) at 172.55°.

In summary, none of the LNAV/waypoint routes have acceptable figures of merit, nor does there appear to be a central peak. Therefore, the MH370 SIO Route is not a LNAV/waypoint route.

10.3 Constant Magnetic Track Results

Figure 11(c) displays the Constant Magnetic Track results. There is a central peak feature, about 1/2° wide, within a region of interest about 1° wide near 181° magnetic track. Figure 12 is an enlarged view of Figure 11 (c).

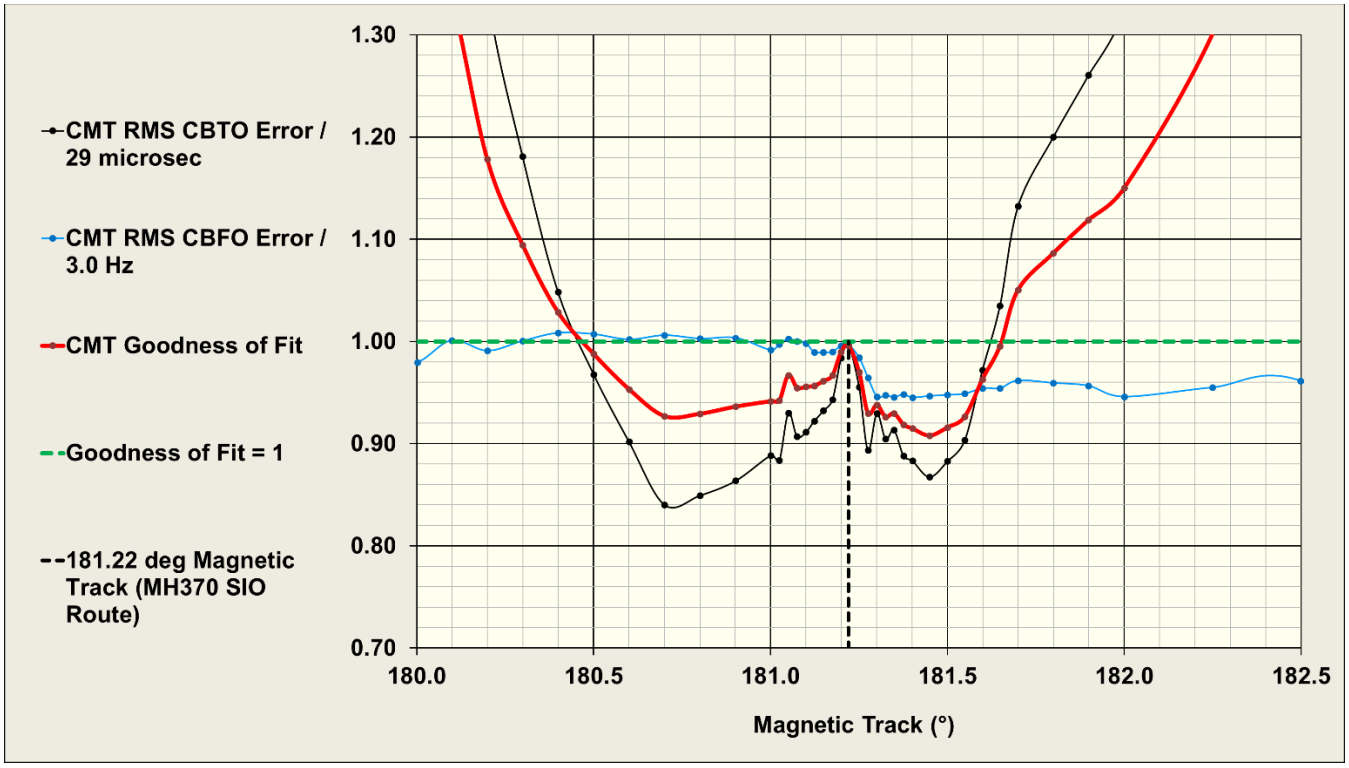

Figure 12. Constant Magnetic Track Plot Contains MH370 SIO Route

The general consistency of Figure 12 with Figure 10 is readily apparent. The CBTO errors rise from a minimum of 0.84-0.86 on the sides to a central peak value very close to 1.0. Note also that there is a step downward of 5% in the CBFO errors that is aligned with the bearing of the central peak feature in the CBTO residuals. This peak occurs

at 181.22°. The central lobe is quite narrow (≈ 0.1°), so the bearing angle is determined with a high degree of precision.

One can see something akin to "grating lobes" in the CBTO central peak, wherein fairly large changes in residuals occur over very small bearing angle changes. This is caused by the "coherence" of the five CBTO values I am fitting. They are coherent (i.e., correlated) because they belong to the same correct route. If there were many more BTO data points, the central peak would probably be smoother in shape, approaching a gaussian function. Still, the lobed structure seen in Figure 12 within the central peak feature is another indicator that this is the correct MH370 SIO Route. Only in this special case are the data sufficiently "coherent" to produce sidelobes.

The CBTO and the CBFO residuals both show a definite improvement in the fitting residuals at 181.22° by being close to the ideal 100% level. The reason for the CBFO errors being different from 1.0 at the "incorrect" bearings is that the systematic errors dominate, because the CBFO noise is quite low. However, because the CBFOs are relatively insensitive to bearing, a change of several degrees is needed to produce a demonstrable degradation in the CBFO fitting residuals. Within the region of interest, the CBTO errors are generally slightly low at the incorrect bearings because the routes there are being fit partially to the CBTO noise. Only at the "correct" MH370 bearing are both the CBTO and the CBFO errors consistent with their normalized expected values (=1.0).

In order to declare 181.22° CMT as the MH370 SIO Route, it must additionally be demonstrated that it is unique. CTT, LNAV/waypoints, and CMH have no central peaks, so they are eliminated from consideration. However, the CTH curve shows two weak central features, which will be discussed in the next section.

Note that the CMT altitude (FL336) in Table 2 is slightly lower than the estimated radar-track altitude (FL340-350). This implies a slight descent was made between 18:22 and 19:41, possibly at the same time as or, more likely, before the FMT.

For the Constant Magnetic Track mode, I computed route fits for many closely-spaced bearings (see Figure 12) to search for a signature similar to that shown schematically in Figure 10. One must look on a very fine scale in bearing or the tell-tale signature can easily be missed entirely. Indeed, that is exactly what happened in previous route searches. Two basic methods were used previously. In one method, the route fits were examined using integer degrees. As shown in Figure 12, the actual MH370 route has a mean estimated bearing of 181.22°, so it is not precisely located at an integer bearing (nor should one expect it to be, because of the imprecision of AFDS control over long time periods for non-waypoint navigation methods). In addition, the signature is very narrow, being only about 1/2° in width, so a search at 1° intervals may not detect the central peak of the correct route.

In a second method previously used, the bearing was allowed to vary while the CBTO and CBFO residuals were minimized. This second strategy also leads to non-detection of the true route, because even if it started at the correct bearing (on the central peak at 181.22°), it would necessarily move off to one side or the other to find lower RMS CBTO/CBFO residuals. Another flaw in previous methods is that the lateral navigation error was neglected. Effectively, that assumes a magnetic track is perfectly followed, with no deviations off the theoretical curved path. The effect of this (incorrect) assumption, is that the CBTO errors will be overestimated. However, because of the CBTO noise fitting that also occurs (reducing the residuals), the two effects somewhat compensate one another, and the RMS residuals are not too different from the CBTO noise alone. However, that process is flawed for two reasons, and coincidentally the residuals might appear reasonable, but the correct route still cannot be identified using that method.

10.4 Constant True Heading Results

Figure 11(d) shows the CTH results. Fitting constant-heading routes is more difficult because one must synthesize four cross-track wind errors in addition to the ten variables for the five handshake positions. This requires significantly longer computer run times, approximately 1 hour for a new route without a good initial set of parameter values. Subsequent runs, with starting points from a nearby (< 1°) solution, require about ½ hour to converge.

Figure 11(d) shows a broad region of interest at 175°-179° true heading. There are also two weak central features for the CBTO and GOF curves. The lack of strong lobed structure at a high angular frequency indicates less than complete coherence, but these two features have many of the characteristics of the correct route solution. The question is, why are there multiple central peaks, one in the CMT plot [Figure 11(c)] and two weak ones in the CTH plot [Figure 11(d]? How is this possible, since two different lateral navigation methods are used?

The answer is simple. It is because all three cases are essentially the same route. Figure 13 shows the three routes (181.2° CMT, 177.4° CTH, and 176.3° CTH) from 19:41-00:19. The black line is the CMT route. The green and blue lines are the CTH routes corresponding to the two central peaks in Figure 11(d). Notice the high degree of overlap, especially from 19:41 (the tops of the routes) through 21:41. The routes then diverge, but only slightly, at 22:41 through 00:19. The pair of CTH routes nicely bracket the CMT route. I conclude that all three features are caused by the true route correlation contained in the satellite data. Clearly, though, only the 181.22° CMT is the correct MH370 SIO Route. The pair of nearly identical CTH routes my method also identified are a result of the similar curvatures of the CMT and CTH routes under these particular conditions.

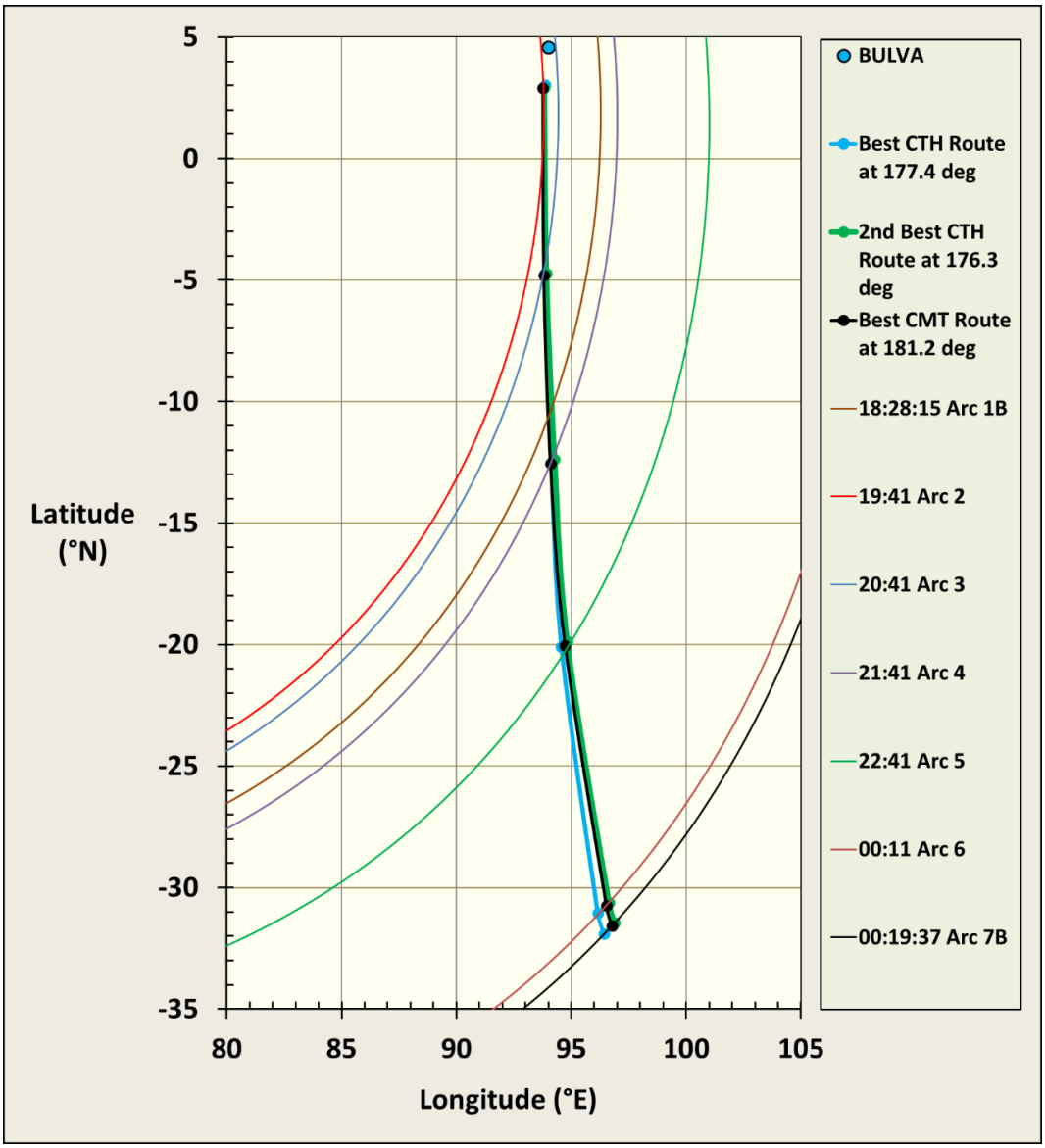

Figure 13. Comparison of Best-Fit CMT and CTH Routes

On this particular night, and in this particular location, the strong westerly crosswinds cause a Constant True Heading route to curve eastward. Similarly, a Constant Magnetic Track route would also curve eastward, not

because of crosswinds, but instead because of the eastward curvature of the magnetic variation in the SIO. It is purely coincidental that these disparate effects happen to closely mimic each other, but it does serve a useful purpose in this analysis. It demonstrates that the (three) central peaks detected in my route analysis are caused by the satellite data set (which is common to both the CTH and CMT routes), not by GDAS crosswinds (affecting only the CTH fit) or by the 2005 magnetic variation table (affecting only the CMT fit). This second and third detections of the correct route, using a different navigation method, clearly demonstrate that the central peak is a feature of the satellite data set, not some vagary of the wind field or the magnetic variation.

The better fit to the correct route is the CMT result. It has lower residuals, strong "sidelobes" indicating a high degree of coherence, and a central peak Goodness of Fit = 1.0. The two CTH detections have central peaks with a GOF ≈ 1.5, and, therefore, those routes are close to, but are not, in fact, the correct MH370 SIO Route. Only the 182.2° CMT route is the correct one for MH370.

10.1 Constant Magnetic Heading Results

Figure 11(e) shows the fitting residuals for the Constant Magnetic Heading route. In this case, the eastward curvature is extreme, because it includes the eastward drift due to winds from the west, plus the eastward curvature of the magnetic variation. As a result of this very large curvature, the route fits are generally poor. The ranges between handshake arcs are simply too variable to match closely any air speed profile used in a B777 with auto-throttle control.

10.2 Summary of Route Identification Process and Result

To summarize, the optimization of the route at a fixed average bearing minimizes an Objective Function by finding five pairs of latitude/longitude so that the RMS wind error, the RMS lateral navigation error, and the mean bearing are tightly controlled at their expected values, while simultaneously minimizing the RMS CBTO and CBFO errors. When both the normalized CBTO and CBFO errors = 1, and when they are significantly lower than 1 at nearby bearings, the correct route signature has been found, and the correct route has been identified. There should be only one such case, and I have found only one, a Constant Magnetic Track at 181.22°.

11. Details of MH370 SIO Route

11.1 Fitting Errors

Figure 14 summarizes the primary fitting residuals for the 181.22° CMT route. The CBFO and CBTO errors are 100% (= 1.00). The lateral navigation errors, along-track wind errors, and the cross-track wind errors are all within 1% of their desired values. The MEFE time is within ½ minute of its desired value.

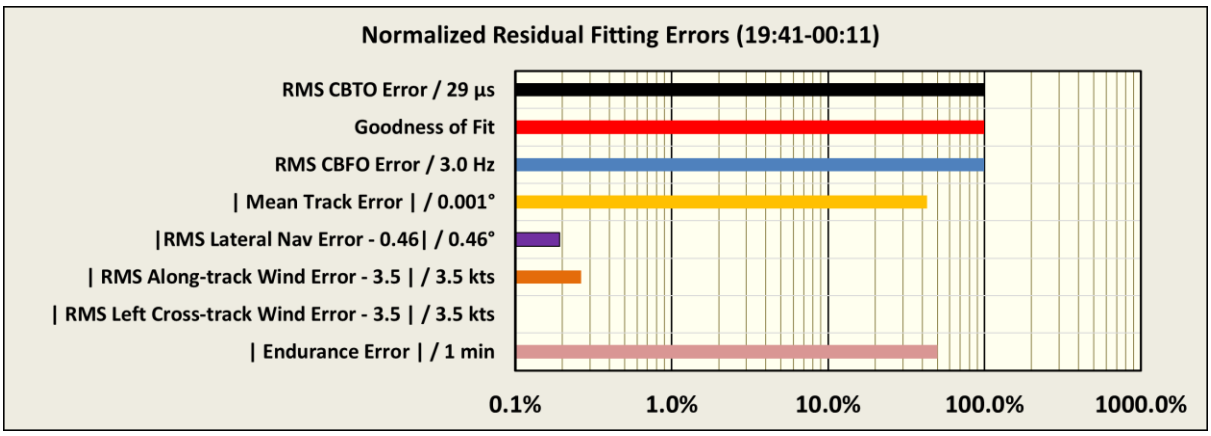

Figure 14. Residual Fitting Errors for MH370 SIO Route

Figure 15 shows the fitting residuals for the two route extensions, one back to 19:00 from 19:41, and the other forward from 00:11 to 00:19.

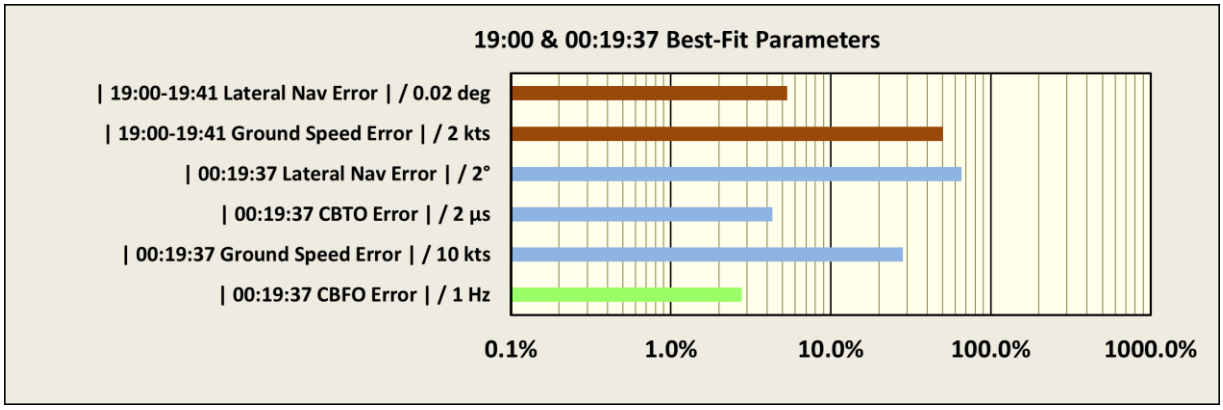

Figure 15. Residual Fitting Errors for Extensions of MH370 SIO Route

11.2 Route Parameters

Table 3 provides the principal parameters of the best-fit MH370 SIO route at the handshake times corresponding to the CBTO "Arcs" #2-7, plus the two extensions.

Table 3. MH370 SIO Route Parameters at Handshake Times

Handshake		Position (°)		Flight Level	Geometric Altitude (ft)	Aircraft Weight (1,000 kg)	True Track (°)	Ground Speed (kts)	Rate of Climb (fpm)	2005 Magnetic Variation (°)	Magnetic Track (°)	GDAS Weather Data at Lat/Lon/FL/UTC			CBTO (µs)			CBFO (Hz)		
Arc #	UTC	Latitude	Longitude									Δ_{SAT} (C)	Wind Speed (kts)	Wind Direction [From] (°)	Predicted	Observed	Error	Predicted	Observed	Error
---	19:00:00.0	8.160	93.768	336	34,899	200.9	180.00	462.4	0	-1.08	181.08	11.2	7.6	262.7	11,739		---	92.5		---
2	19:41:00.0	2.881	93.768	336	34,876	200.7	179.86	460.1	0	-1.36	181.22	11.0	18.8	82.7	11,507	11,500	7	106.6	111.4	-4.8
3	20:41:02.0	-4.809	93.806	336	34,968	194.6	178.79	459.3	0	-2.19	180.98	11.8	12.4	63.0	11,767	11,740	27	141.5	141.4	0.1
4	21:41:24.0	-12.546	94.095	336	34,979	188.6	176.59	454.6	0	-3.89	180.48	11.9	17.8	59.2	12,787	12,780	7	167.3	168.4	-1.1
5	22:41:19.0	-20.034	94.731	336	34,919	182.9	173.34	441.6	0	-6.80	180.14	11.3	4.7	249.6	14,484	14,540	-56	201.1	204.4	-3.3
6	0:11:00.0	-30.741	96.524	336	34,255	174.8	168.41	394.5	0	-14.11	182.52	5.5	74.7	275.9	18,054	18,040	14	249.3	252.4	-3.1
7B	0:19:37.4	-31.566	96.774	200	21,066	174.4	162.48	316.4	-14,822	-14.82	177.30	9.2	21.1	251.6	18,410	18,410	0	-5.2	-5.2	0.0

RMS of 19:41 - 00:11 Data	28.9	µs		2.99	Hz
Expected RMS Value	29.0	µs		3.00	Hz
Normalized RMS Value	0.996	---		0.997	---

Goodness of Fit	0.996

The blue cells in Table 3 show the residual CBTO errors, and the green cells show the residual CBFO errors for Arcs #2-6 (19:41-00:11) which were used for determining the SIO route. The yellow cells show their normalized RMS values, and the turquoise cell shows the overall Goodness of Fit parameter.

Table 4 shows the averages of key route parameters for each of the four "legs" of the MH370 SIO Route between the handshake arcs. The blue cells in Table 4 show the along-track wind errors found by the differences between the model predictions (based on the B777-200ERE air speed model and the GDAS wind field) and the values calculated using the latitude/longitude positions of the leg ends. The RMS along-track wind error is tightly constrained to be within 1% of 3.5 kts. The green cells in Table 4 are the lateral navigation errors for each leg. Again, their RMS value is tightly constrained to be within 1% of 0.46°.

Table 4. MH370 SIO Route Average Leg Parameters

Leg			Average Model Airspeed		Average GDAS Δ_{SAT} (C)	Average GDAS Along-track Wind Speed (kts)	Model Ground Speed from Vector Sum of Air and Wind Speeds	Average Ground Speed from Lat / Lon (kts)	Along-track Wind Error (kts)	True Track (°)		
#	From (UTC)	To (UTC)	KTAS (kts)	Mach (---)						From Lats / Lons	From CMT Commanded Magnetic Bearing	Error
1	19:41:00.0	20:41:02.0	455.8	0.767	11.1	3.9	459.5	458.9	-0.6	179.71	179.44	0.27
2	20:41:02.0	21:41:24.0	448.9	0.754	11.4	6.9	455.6	459.6	4.0	177.87	178.18	-0.31
3	21:41:24.0	22:41:19.0	441.4	0.741	11.8	3.3	444.6	449.6	5.0	175.31	175.87	-0.56
4	22:41:19.0	0:11:00.0	429.2	0.722	11.6	8.9	436.4	433.5	-2.8	171.37	170.76	0.61
5	0:11:00.0	0:19:37.4	348.9	0.594	8.4	12.3	358.2	355.4	-2.8	165.44	166.76	-1.31

RMS of 19:41-00:11 Errors	3.51	(kts)		0.461	(°)
Expected RMS Value	3.50	µs		0.460	(°)
Normalized RMS Value	1.003	---		1.002	---

11.3 Aircraft Flight Parameters

Figure 16 illustrates the aircraft flight parameters from 17:07-00:19.

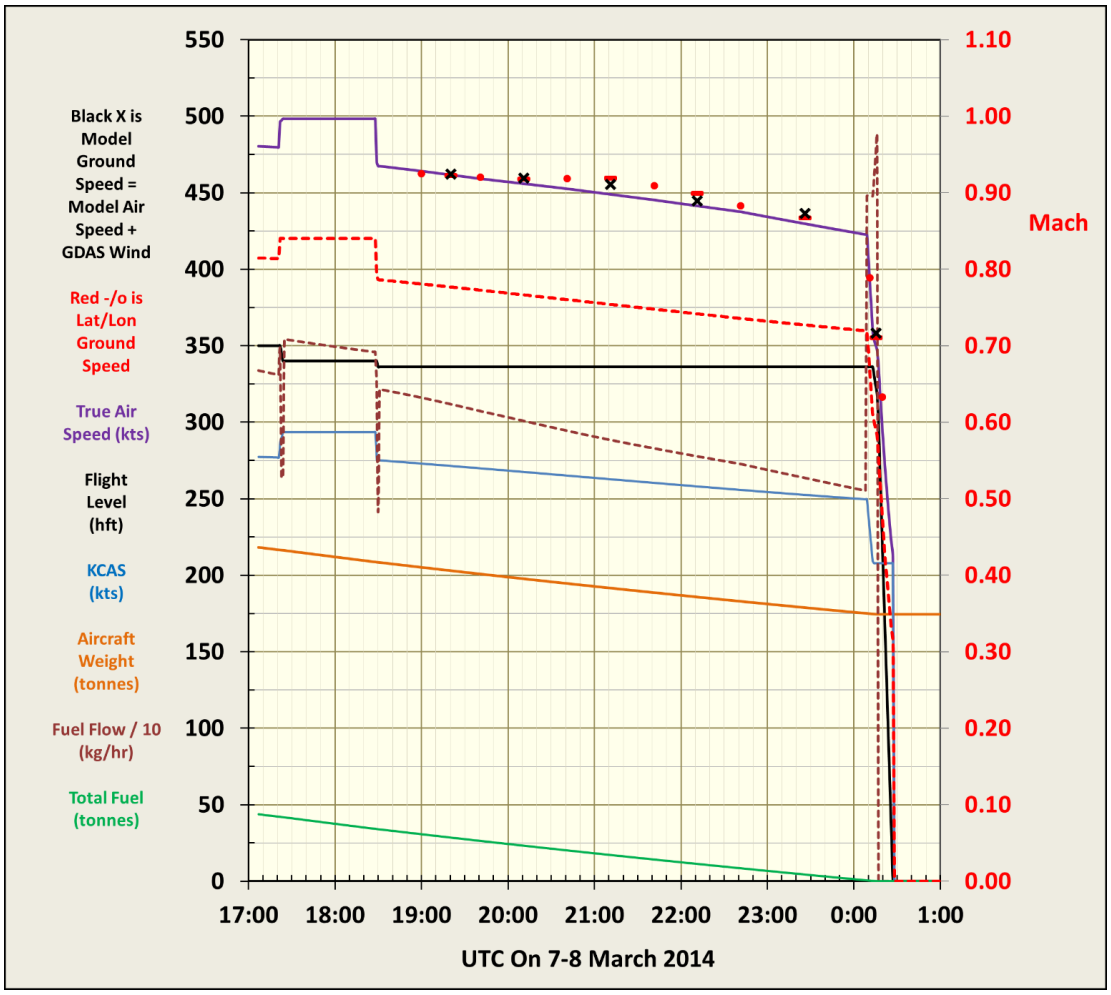

Figure 16. Flight Parameters for MH370 SIO Route

11.4 MH370 SIO Route Map

Figure 17 shows a map of the MH370 Route from 18:20 – 00:19. The predicted 7th Arc location is 31.57°S, 96.77°E.

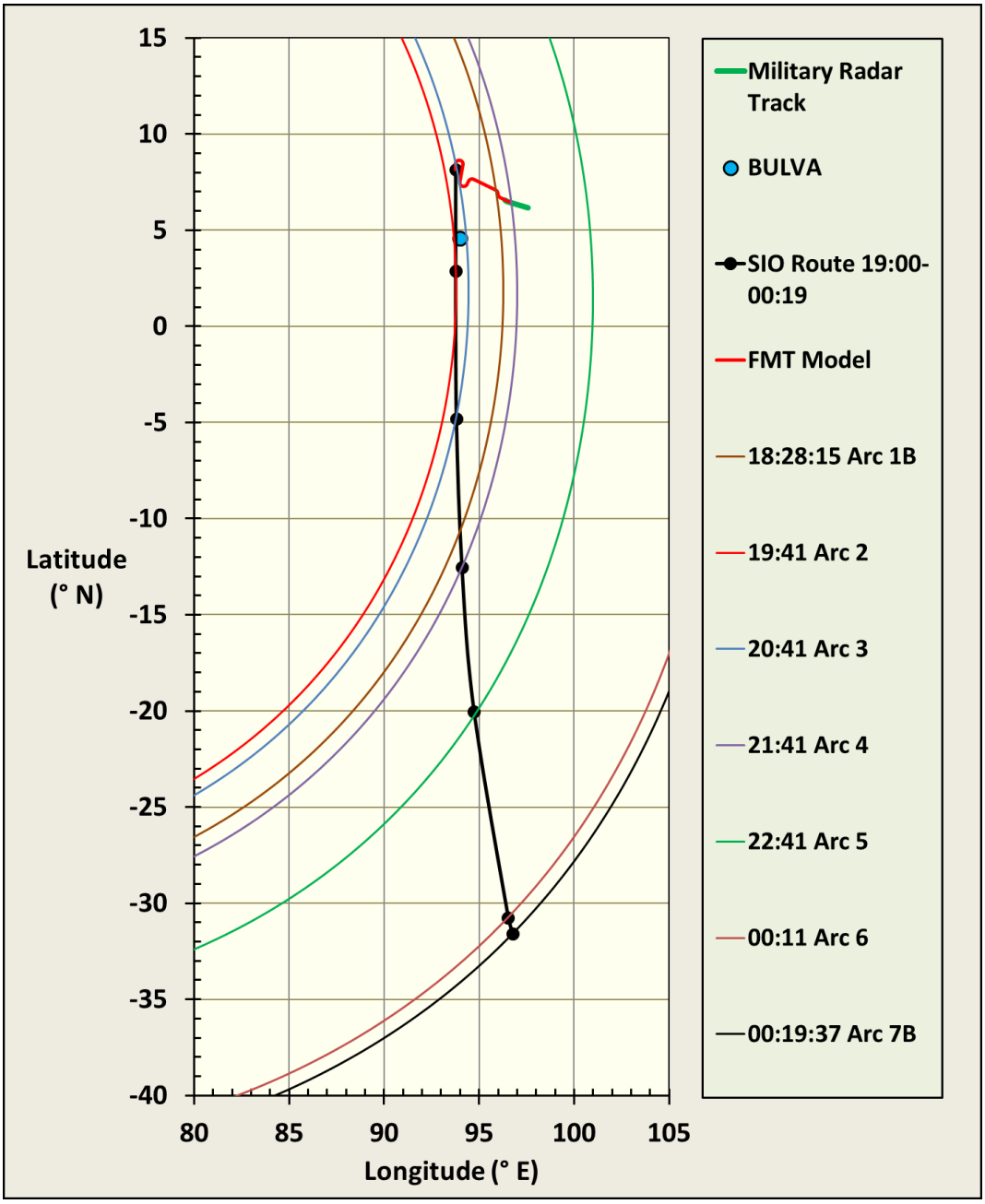

Figure 17. MH370 SIO Route

12. MH370 Route from 18:22 – 19:41

The SDU was repowered circa 18:22, leading to a satellite data link log-on at 18:25 [9]. The left AC bus may have lost power near the initial diversion time of 17:22. The 18:25 log-on triggered a series of BTO and BFO measurements from 18:25-18:28. The first few BTOs then were affected by the warm-up transient in the Oven-Controlled Crystal Oscillator (OCXO) that provides the transmitting frequency reference for the SDU. It is possible to estimate these corrections, and the resulting CBFOs plus the relatively unaffected CBFOs later on indicate a 15NM right offset maneuver (i.e., a lateral offset Contingency Procedure, or LOCP) from airway N571 was performed circa 18:25, following the airline's Contingency Procedures shown in Figure 18 [27].

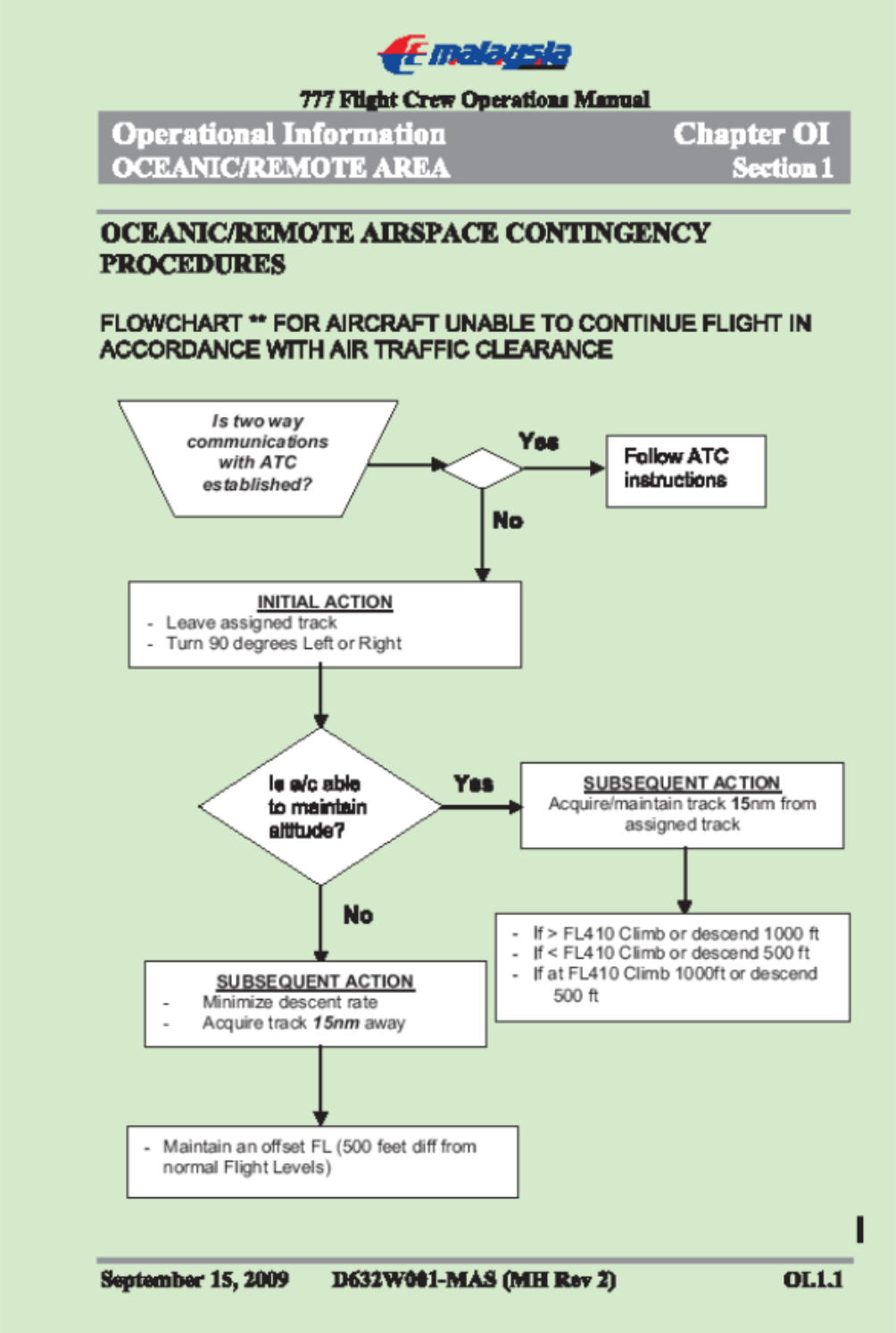

Figure 18. Malaysia Airlines Contingency Procedures for Lost ATC Clearance

The observed ground speed over the military radar track is well-matched by M0.84 at FL340 [28]. Prior to reaching IGARI circa 17:21, MH370 was flying at FL350 using the Flight Plan speed setting (ECON with Cost Index = 52). Subsequent to the diversion, the speed was increased and it appears the flight level was reduced to the next lower "even" FL340. The flight level is normally even when flying westward, so changing from an "odd" FL350 (traveling eastward near IGARI) to an "even" FL340 would be a normal practice. At 18:25 the 15 NM right LOCP was begun. Figure 18 shows the Contingency Procedures flow chart for Malaysia Airlines when ATC communications and clearance are lost.

Note that, if the altitude can be maintained, the first step in the Contingency Procedures is to acquire and maintain a track offset by 15 NM. In this case I know (from the CBTO/CBFO data) that the aircraft turned to the right. Thus, there is a good correspondence between the pilot actions then and the first step of the Contingency Procedures. The second step is to climb or descend by 500 feet (if the current flight level is < 410, which it is when at ≈ FL340) after the offset track is established circa 18:28. In this case, it seems the choice was made to descend 500 feet, since the SIO route indicates FL336 was used. The difference between FL336 and FL335 in my speed and fuel flow models is too small be to be considered meaningful. Thus, the SIO route was most likely flown at 33,500 feet (FL335). Therefore, the second step of the Contingency Procedures also seems to have been implemented by the pilot in charge (PIC). To summarize, the PIC made the 15 NM right offset circa 18:25 and then reduced altitude by 500 feet circa 18:29, both actions being in accordance with the airline Contingency Procedures for the case when ATC clearance cannot be obtained.

Figure 19 is a map of the area containing the flight path from last radar contact at 18:22 through the Handshake Arc #2 location at 19:41.

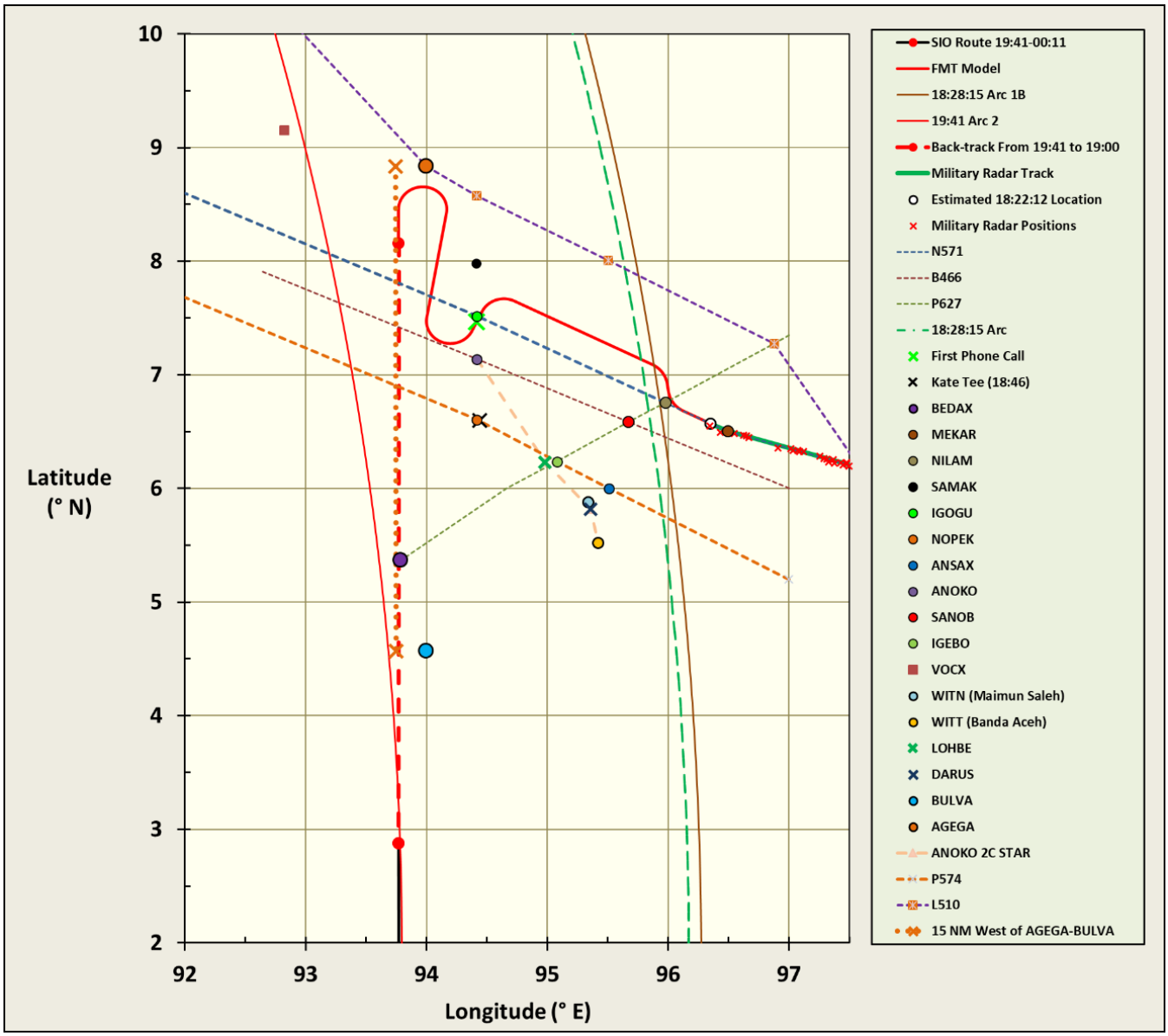

Figure 19. MH370 SIO Route Near FMT

The back-track from 19:41 to 19:00 is shown as the vertical dashed red line to the left of center in Figure 19. The true bearing from AGEGA to BULVA is 179.96° at a range of 254.9 NM. The magnetic variation at a point 15NM west of AGEGA is -1.05°; it is -1.26° when 15 NM west of BULVA. Therefore, the magnetic track 15 NM west of AGEGA is 181.01° [= 179.96° – (-1.05°) = 181.01°], and it is 181.22°[= 179.96° – (-1.26°) = 181.22°] when 15 NM west of BULVA. Since the MH370 SIO Route has a best-fit magnetic track of 181.22 degrees, it is consistent with having been selected, using TRACK HOLD, at a point near BULVA. The simplest means to get a constant magnetic track is to use TRACK HOLD on the MCP, and it appears that was done at a point near 15 NM west of BULVA at a time near 19:28 (or perhaps somewhat earlier when between AGEGA and BULVA).

For the MH370 SIO Route, the best-fit back-track position at 19:27:57 is 14.1 NM due west of BULVA, which is only 0.9 NM from a nominal 15 NM right lateral offset position (shown as the orange dotted line in Figure 19). The best-fit back-track bearing of 181.22° magnetic matches exactly the magnetic track at this location when following the AGEGA-BULVA track (179.96° true minus the magnetic variation of -1.26° = 181.22° magnetic). Thus, there is a simple set of waypoints (AGEGA and BULVA) which, when followed, can lead to the MH370 181.22° CMT route after 19:28. In addition, the backward extension of the best-fit SIO route is consistent with the 15 NM right lateral offset established at 18:25 near NILAM and continued though waypoint BULVA at 19:28.

For comparison purposes, the predicted back-track position at 18:55:00 is 13.6 NM west of AGEGA, and the predicted magnetic track there is 181.01°. Therefore, the best-fit magnetic track is in better agreement with the TRACK HOLD occurring near BULVA than near AGEGA, although this TRACK HOLD action could have been done at any point between AGEGA and BULVA. It does not seem likely that the CMT route was the result of a route error in the FMC (such as “End of Route” or “Route Discontinuity”). The reason for this is that the default lateral navigation method after such a FMC error is a constant heading, not a constant track (based on simulator runs).

The solid red line in Figure 19 is a somewhat speculative FMT Model prediction connecting the radar track end at 18:22:12 to the back-track beginning at 19:00:00. There are three turns. The first turn is to waypoint ANOKO (while maintaining the 15 NM right lateral offset). This produces a 206° true track at 18:40, matching the phone call CBFOs then at MRC speed [29].

The second turn begins toward AGEGA when ANOKO is reached. The third turn is to BULVA when in the vicinity of AGEGA. This set of turns matches the back-track position at 19:00 near AGEGA travelling due south. The exact path near AGEGA depends on when the speed reduction occurred from M0.84 (across the military radar track) to MRC (from 19:41 onward). In Figure 19 MRC was commanded at the same time as the altitude was reduced by 500 feet (circa 18:29). If the slow-down occurred later, then the FMT Model allows a path circling around AGEGA instead of turning just before reaching it.

At 19:10 the best-fit back-track of the MH370 SIO Route passed about 40 NM due west of possible eyewitness Katherine Tee [30]. 9M-MRO would have been at 33,500 feet, traveling N-S and probably with all exterior lights on (which is another step in the Contingency Procedures). The timing of her sightings, just before a jibe of her sailboat at 19:15, of two high-altitude aircraft fits rather well. The direction does not, since she says they were headed north. The elevation angle would have been 8 degrees above the horizon at closest approach, whereas she describes 50°. The night was clear, and she would not have had any difficulty in seeing 9M-MRO for at least 10 minutes. If Katherine Tee did see 9M-MRO, it probably was not the low-altitude aircraft she also described seeing a few minutes later. This is not certain, however, since the SIO route fit only begins at 19:41, about 30 minutes after her sightings, and it is not impossible for 9M-MRO to have descended to a much lower altitude between 18:29 and 19:10 and then climbed back to FL335 between 19:15 and 19:41.

13. MH370 Timeline

Table 5 is a timeline of significant MH370 events from take-off until the end of the flight. The turns to ANOKO, AGEGA, and BULVA are speculative, and they are intended simply to illustrate one path that seamlessly connects the fairly well known 18:29 position to the best-fit SIO Route.

Table 5. MH370 Timeline

Event	Time (UTC on 7-8 March 2014)	Notes	Track (° True)	Flight Level (hft)	Air Speed	Lateral Offset (NM Right)
Take-off from WMKK	16:42:00	• 9M-MRO left Kuala Lumpur International Airport (WMKK) bound for Beijing as Malaysia Airlines Flight MH370	---	---	---	None
Last ACARS report sent from aircraft	17:06:43	• Last aircraft status and fuel report sent • This is the starting point for my fuel model calculations	26	350	ECON with Cost Index = 52 (Flight Plan)	
Diversion from Flight Plan	17:21:13	• Began after shortly passing IGARI • Radar transponder and radios became nonresponsive • Possible loss of left AC Bus • Rapid return to Malaysia begun	59			
Diversion turnaround completed	17:26:13	• Standard practice is to use "even" Flight Levels when course is west of N-S line • Descended 1,000 feet to next even altitude (FL340) • Speed increased to M0.84 for rapid return to Malaysia	237	340	Mach 0.84	
Pass near Kota Bharu (WMKC)	17:35:57	• No descent or landing attempt at this closed airport • Possibly flying using MCP to set heading				
Pass near Penang International Airport (WMKP)	17:52:35	• No descent or landing attempt at this primary alternate airfield • First Officer's mobile phone connected to a cell tower at 17:52:27 • Possibly flying on autopilot but using MCP to set heading • Passed near waypoint KENDI a few miles south of the airport	237			
Pass Pulau Perak	18:02:59	• Eyewitness (military) reported a high flying aircraft passed near this island military base	286			
Last military radar contact	18:22:12	• Per ATSB, aircraft was 10 NM Past MEKAR on Airway N571	296			15 NM
Power restored to SDU	18:22:27	• Time estimated based on SDU boot time of 3 minutes from a cold start • Power probably restored to Left AC bus				
Begin Lateral Offset Contingency Procedure (LOCP)	18:24:01	• Malaysia Airlines has a Contingency Procedure if Air Traffic Control clearance is lost • First step is 15 NM offset, then 500 ft altitude change, then turn on all exterior lights • Begin first (right) turn to a new course of ≈ 351° true to reach 15 NM to right of and parallel to Airway N571				
Renewed satellite communications	18:25:27	• First SDU log-on to satellite network after Diversion	347			
Begin 2nd turn of LOCP	18:26:08	• Second turn of LOCP begins at 351° and ends at 296°	351			
LOCP completed	18:27:42	• Resume NW course parallel to N571, but offset 15 NM to the right	296	335	Maximum Range Cruise (MRC; ECON with CI=0)	
SDU Handshake #1	18:28:15	• IFE sets up ground connection for BITE application • I use this handshake for Arc #1 because the BFO then is less affected by the OCXO warm-up transient error				
Change altitude 500 feet per Contingency Procedure	18:29:00	• Airlines Contingency Procedure is to change altitude by 500 feet • In this case, it appears a descent was made from FL340 to FL335 • Airlines procedure is also to turn on all exterior lights				
Slow down to Maximum Range Cruise (ECON with Cost Index = 0)	18:29:00	• Speed change may have occurred simultaneously with 500 ft descent, but could have occurred any time from 18:29-19:00 • New air speed is M0.796				
Turn to waypoint ANOKO	18:37:20	• ANOKO is the first waypoint in the ANOKO2C Standard Terminal Arrival Route (STAR) for the nearest airport with a sufficiently long runway for a B777 (WITT in Banda Aceh, Indonesia) • Retain 15 NM right lateral offset				
First satellite phone call	18:39:55 - 18:40:56	• Malaysia Airlines places call to 9M-MRO • Call is not answered • Track is 206° true toward ANOKO	206			
Turn to waypoint AGEGA	18:41:10	• Turn to 10° true • Retain 15 NM right lateral offset • Purpose is uncertain, but is in general direction of airport VOCX on Car Nicobar				
Turn to waypoint BULVA	18:52:45	• Turn to 179.96° true • Retain 15 NM right lateral offset • Now flying away from land	10			
Enter Track Hold in MCP	18:55 - 19:30	• NORM/TRUE switch is usually in NORM position, leading to magnetic bearing reference • Setting TRACK HOLD causes Constant Magnetic Track at current bearing of 181.22° magnetic • BULVA passed at 19:30 • Purpose is uncertain, but path avoids land and reaches SIO	179.958			Not used
Possible eyewitness sighting	19:12	• Katherine Tee's report of the first aircraft she sighted (not the low-altitude one) is consistent in some, but not all, respects with the expected appearance of 9M-MRO following my notional FMT route from 18:29-19:41 • Katherine Tee reported the first aircraft she saw (at 18:50-19:10 UTC) was at a very high altitude west of her position and had flashing white lights • Using my notional FMT route, at 19:10 9M-MRO was about 40 NM due west of Kate Tee, at 8° elevation angle				
SDU Handshake #2	19:41:00	• SDU Handshake #2				
SDU Handshake #3	20:41:02	• SDU Handshake #3				
SDU Handshake #4	21:41:24	• SDU Handshake #4				
SDU Handshake #5	22:41:19	• SDU Handshake #5				
Second unanswered satellite phone call	23:14:01 - 23:15:02	• Malaysia Airlines again calls 9M-MRO, but call is not answered • 60 minute timer at ground station for check-in is reset				
Right engine fuel exhaustion	00:09:30	• Estimated right engine flame-out time using my endurance model • Right engine consumes 2% more fuel than left engine in cruise and flames out first				
SDU Handshake #6	00:11:00	• SDU Handshake #6		335	Decelerating; Engine Inoperative	
Left engine fuel exhaustion	00:17:30	• Left engine flames out • Fuel tanks are empty • APU start attempted using fuel in lines • Ram Air Turbine deployed		Descending slowly		
APU restores power to SDU	00:18:30	• Estimated to occur 1 minute before first transmission for a hot start	Unknown		High Deceleration; Both Engines Inoperative	
SDU begins to log in after power is restored	0:19:29	• SDU reboots in one minute after power is restored • Rate of Descent is 4,600 fpm per BFO		Descending rapidly		
Last aircraft data transmission	00:19:37	• My SDU Handshake #7 • Partially controlled flight • Rate of descent is 15,000 fpm per BFO		≈ FL200		
Next expected aircraft transmission	00:21:00	• Next message expected at ≈ 00:21 was not received fom SDU	Loss of signal may indicate aircraft fell into the sea prior to 00:21			

14. Recommendation

I recommend Ocean Infinity search the 10,300 km^2 zone within ± 25 NM of the 7th Arc (at 20,000 feet) and within ± 30 NM along the arc from my predicted location at 31.57°S, 96.77°E. That zone, shown in Figure 20, is in Site 2 Extension Area 3, and it conservatively encompasses the expected uncertainties in my predicted location.

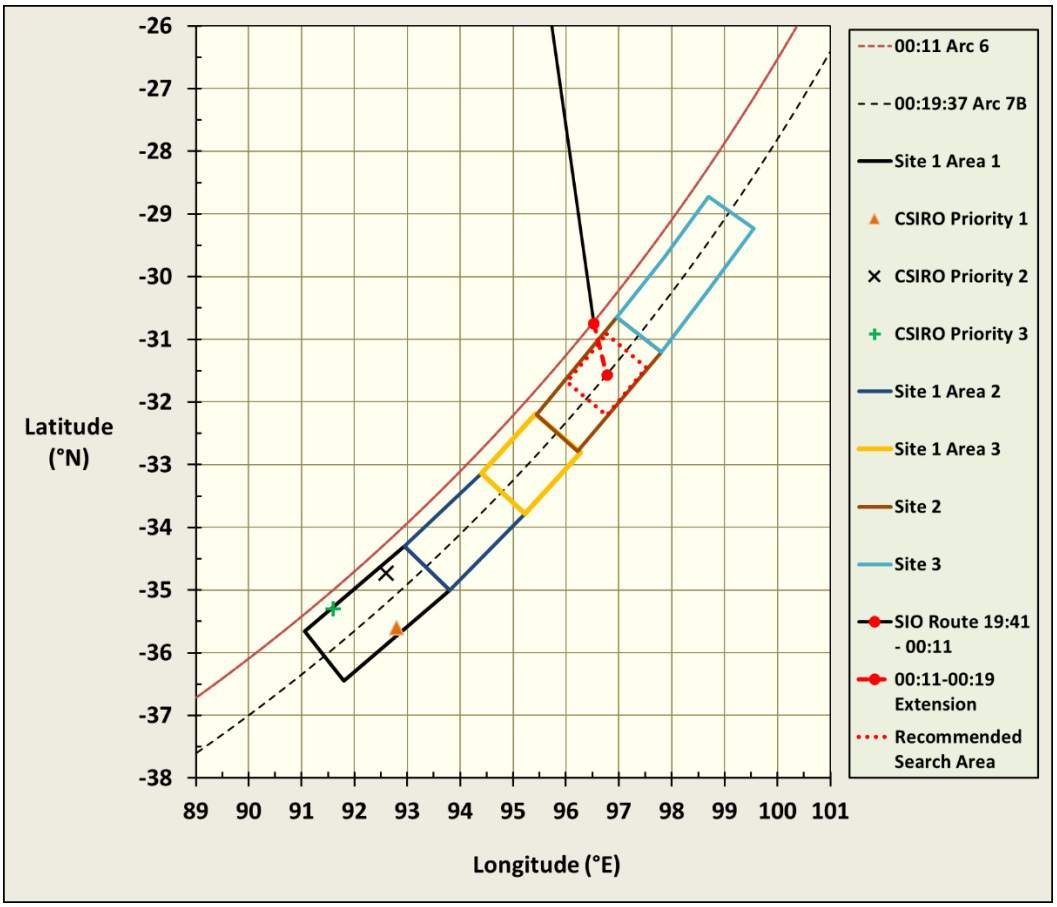

Figure 20. MH370 SIO Route Terminus and Recommended Search Area

15. Acknowledgment

This work was done in the hope that the families of MH370 victims might learn more about what happened to their loved ones. In addition, aviation safety may be improved for the benefit of the traveling public.

16. References

[1] Inmarsat, "Update to Signalling Unit Logs," December 2014. [Online]. Available: https://www.atsb.gov.au/publications/2014/mh370-update-to-signalling-unit-logs/.

[2] Smart Cockpit, "Boeing B777 Systems Summary (Automatic Flight)," 16 February 2008. [Online]. Available: https://drive.google.com/file/d/18y1j_V2SpvKan785BaIvvlzhK_Z_-4ih/view?usp=sharing.

[3] Honeywell Aerospace Electronic Systems, "B777 Flight Management System Pilot's Guide," 12 October 2014. [Online]. Available: https://drive.google.com/file/d/1uHJgtGojMK4cBzdpxRqtOd_xExOs-onL/view?usp=sharing.

[4] ATSB, "First Principles Review (Figure 14)," 2 November 2016. [Online]. Available: www.atsb.gov.au/newsroom/2016/mh370-first-principles-review-and-csiro-reports/.

[5] Malaysia, "“MH370 OPERATIONAL SEARCH UPDATE #1”, Period 21-28 JANUARY 2018, Diagram 1," 30 January 2018. [Online]. Available: http://mh370.gov.my/en/mh370-underwater-search-2018#.

[6] National Oceanic and Atmospheric Administration, "Global Data Assimilation System," 2018. [Online]. Available: https://www.ncdc.noaa.gov/data-access/model-data/model-datasets/global-data-assimilation-system-gdas.

[7] NOAA, "GDAS Weather Data," 2018. [Online]. Available: https://earth.nullschool.net/#2014/03/08/0000Z/wind/isobaric/250hPa/overlay=temp/orthographic=108.54,-20.30,1361/loc=96.770,-31.570.

[8] B. Ulich, "MH370 Weather Data," 7 February 2017. [Online]. Available: https://drive.google.com/file/d/0BzOIIFNlx2aUcEY5YkJtY0lpckE/view.

[9] B. Ulich, "OCXO Transient Errors and 18:25 LOCP Fit," 18 January 2018. [Online]. Available: https://drive.google.com/file/d/1d8Td73ayKCQyRzGwUBEKCPyYA0XYJtz2/view?usp=sharing.

[10] ATSB, "MH370 - Definition of Underwater Search Areas (Figure 6)," 10 December 2015. [Online]. Available: https://www.atsb.gov.au/media/5747317/ae2014054_mh370-definition_of_underwater_search_areas_3dec2015_update.pdf.

[11] B. Ulich, "9M-MRO Fuel Flow and Endurance Models," 4 November 2017. [Online]. Available: https://drive.google.com/file/d/1Wt9DOU0Z53W7NERzSsK2sxcyrojmN7Sq/view?usp=sharing.

[12] B. Ulich, "Comparisons of Observed and Predicted MH370 Endurance," 12 October 2017. [Online]. Available: https://drive.google.com/file/d/0BzOIIFNlx2aUbTlqcjA5bjduUVU/view?usp=sharing.

[13] B. Ulich, "Predicted MH370 Range and Endurance Using Fuel Model V5.4," 23 October 2017. [Online]. Available: https://drive.google.com/file/d/0BzOIIFNlx2aUaFdEUmpKMkxtNDA/view?usp=sharing.

[14] Defense Science and technology Group, Australia, "Bayesian Methods in the Search for MH370 (Page 42)," 3 December 2015. [Online]. Available: https://link.springer.com/book/10.1007/978-981-10-0379-0.

[15] R. M. Police, "MH370 - Folder 5 - Aircraft Record and DCA Radar Data (MH370 Flight Plan)," 2014. [Online]. Available: https://drive.google.com/file/d/0BzOIIFNlx2aUTS1EaUZVVm10WWs/view?usp=sharing.

[16] Defense Science and Technology Group, Australia, "Bayesian Methods in the Search for MH370 (Figure 5.2)," 3 December 2015. [Online]. Available: https://link.springer.com/book/10.1007/978-981-10-0379-0.

[17] Defense Science and Technology Group, Australia, "Bayesian Methods in the Search for MH370 (Table 5.1)," 3 December 2015. [Online]. Available: https://link.springer.com/book/10.1007/978-981-10-0379-0.

[18] B. Ulich, "MH370 CBTO and CBFO Models," 6 November 2017. [Online]. Available: https://drive.google.com/file/d/0BzOIIFNlx2aUV2lQQm96OVJ2OFk/view?usp=sharing.

[19] Australian Transport Safety Bureau, "MH370 - Definition of Underwater Search Areas (AE-2014-054)- Updated 30 July 2015," 26 June 2014. [Online]. Available: www.atsb.gov.au/media/5668327/ae2014054_mh370__search_areas_30jul2015.pdf.

[20] C. Ashton, A. S. Bruce, G. Colledge, and M. Dickinson, "The Search for MH370," January 2015. [Online]. Available: https://www.cambridge.org/core/journals/journal-of-navigation/article/the-search-for-mh370/D2D1C4C99E7BFDE35841CFD70081114A.

[21] B. Weinstein, "Correcting the Effects of Magnetic Variation," Aero Quarterly Q4 2009. [Online]. Available: http://www.boeing.com/commercial/aeromagazine/articles/qtr_04_09/index.html.

[22] National Oceanic and Atmospheric Administration, "Magnetic Declination," 2018. [Online]. Available: https://www.ngdc.noaa.gov/geomag-web/#declination.

[23] D. Thompson, "The Disappearance of MH370," 28 January 2018. [Online]. Available: http://mh370.radiantphysics.com/2018/01/21/the-search-for-mh370-begins-again/#comment-11730.

[24] Malaysia ICAO Annex 13 Satety Investigation Team for MH370, "Updated Factual Information (Safety Investigation for MH370)," 28 March 015. [Online]. Available: http://mh370.mot.gov.my/download/FactualInformation.pdf.

[25] V. Iannello and R. Godfrey, "Possible Flight Path of MH370 towards McMurdo Station, Antarctica," 25 August 2016. [Online]. Available: https://drive.google.com/file/d/1nAyA2wxUqO6gkeCtUOBI0e1RQ7NklMRR/view?usp=sharing.

[26] R. Godfrey, "The Probable End Point of MH370," 12 February 2017. [Online]. Available: https://www.dropbox.com/s/hz0p6e2fqcbecsc/2017-02-14%20Godfrey%20-%20Probable%20End%20Point%20of%20MH370.pdf?dl=0.

[27] Malaysia Airlines, "Oceanic/Remote Airspace Contingency Procedures [Malaysia Airlines 777 Flight Crew Operations Manual; D632W001-MAS (MH Rev 2)]," 15 September 2009. [Online]. Available: https://drive.google.com/file/d/1heAuNkkk7PUFfzcQKymW-fnnyESkVh26/view?usp=sharing.

[28] B. Ulich, "Did MH370 Slow Down Prior to 18:22?," 23 September 2017. [Online]. Available: https://drive.google.com/file/d/0BzOIIFNlx2aUUHdpZnBxazE5aEk/view.

[29] B. Ulich, "MH370 Maneuvers Matching the 18:40 CBFOs (Figure 6)," 18 January 2018. [Online]. Available: https://drive.google.com/file/d/1N3AKqkrh50c0-ovUOloBcSRUpjXwAAIR/view.

[30] K. Tee, "I Think I Saw MH370," 2014. [Online]. Available: http://www.cruisersforum.com/forums/f108/i-think-i-saw-mh370-127132-5.html.

17. Revisions

(1)

18. Publications List

A list of all my MH370 publications, including download links, is available at:

https://drive.google.com/file/d/0BzOIIFNlx2aUS05JcEhsUXprcFE/view?usp=sharing